RESIN TRANSFER MOLDING

Teaching assistant: Valentin Rougier (MXH 144, valentin.rougier@epfl.ch),
Helena Teixidó (MXG 121, helena.teixidopedarros@epfl.ch)

TP Location: MED 3 1119

Suggestion: read the annexes beforehand

Objectives

- Measure unsaturated and saturated permeability of a random glass fabric from a single experiment, following the guidelines in the annexes II and III
    - Emulate a resin transfer molding (RTM) manufacturing process of a composite plate
    - Monitor the impregnation process
- Analyze the results and determine the permeability of the fabric
- Compare saturated and unsaturated permeabilities

Experimental process

- Fabric preparation
    - Calculate the number of layers necessary to manufacture a rectangular panel (laminate) with the desired volumetric reinforcement fraction.
    - Cut the fabric in rectangles of 350 × 100 mm^2.
    - Weigh the fabric
    - Calculate the actual fiber volume fraction V_f
- Mold preparation
    - Open and clean the mold
    - Place the silicone O-ring seal, the metallic frame and the fabric following the schematic plotted in Fig. 1

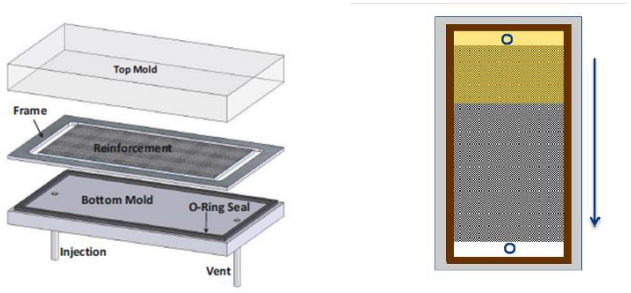

Figure 1. Schematic RTM and permeability set-up

- Test-fluid preparation
    - Degas the test fluid solution for 10 min
    - Prepare the pressure pot
- Prepare the camera
- Perform the injection
    - Record the position of the flow front during impregnation (unsaturated flow)
    - Measure the fluid pressure at the inlet
    - Record the mass of out-coming fluid (saturated flow)

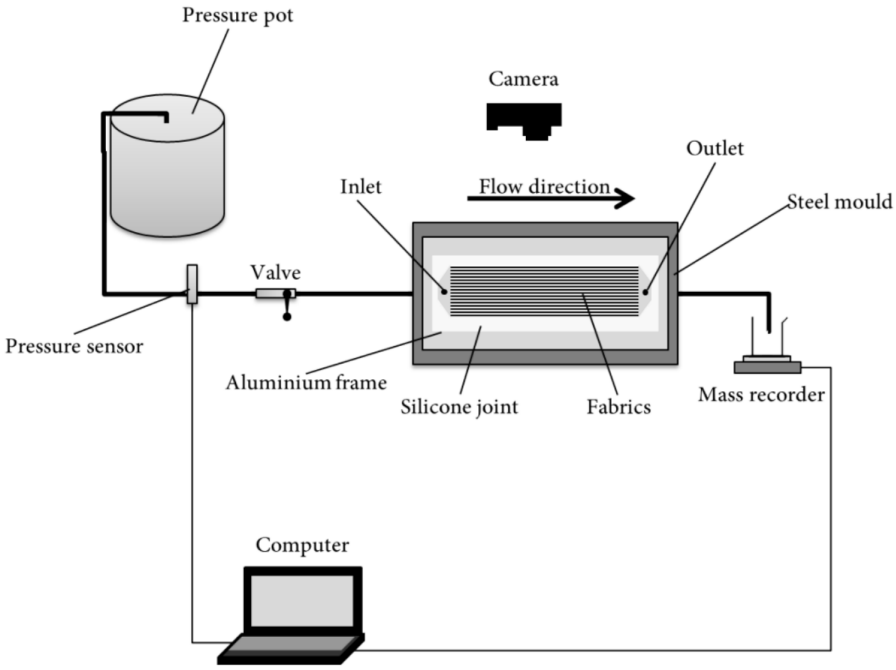

Figure 2. Schematic permeability measurement

Data analysis

- Unsaturated permeability: analyze experimental data (video and pressure datasheet) according to the annex I "Experimental Procedures to Run Longitudinal Injections to Measure Unsaturated Permeability of LCM Reinforcements", paragraph *8.2*
    - Plot squared flow front position evolution in time
    - Determine the slope in the linear range
    - Determine the average fluid pressure at inlet
    - Calculate unsaturated permeability from the experimental data
- Calculate the saturated permeability according to the annex II "Permeability properties of reinforcements in composites", eq. 14.22
    - Calculate volumetric flow rate from mass data

Report

- General introduction on RTM (principles, applications, issues, comparison with other processes etc.)
- Deduce theoretical resin velocity $v(t)$ in unidirectional flow at constant pressure by integration of Darcy's law:

$$(1 - V_f)v = -\frac{K}{\mu}\frac{\partial \mathrm{P}}{\partial \mathrm{x}}$$

with v fluid velocity
V_f fabric volume fraction
K fabric permeability
μ fluid viscosity
$\frac{\partial \mathrm{P}}{\partial \mathrm{x}}$ negative pressure gradient between inlet and flow front

- Compare theoretical and experimental $v(t)$
- Compare saturated and unsaturated permeabilities

Resin transfer moulding (RTM)

(Moulage par transfert de résine)

Et présentation d'autres variantes d'injection de résine à basse pression

Luis Canal, Maria Benavente, LTC, EPFL (2014)

Types de techniques d'injection à basse pression

Cette introduction présente surtout la méthode RTM ainsi qu'une rapide présentation de ses principales variantes.

- Resin Transfer Moulding (RTM)
- Vacuum assisted Resin Transfer Moulding (VARTM)
- Vacuum assisted Resin Infiltration (VARI or RTM Light)
- SCRIMP RTM
- Liquid Compression Moulding

Principe général du procédé RTM

En RTM, un renfort fibreux est préformé ou découpé aux dimensions nécessaires et placé dans un moule (Figure 1). Le moule est ensuite fermé, ce qui compacte le renfort. La résine est injectée à basse pression (<12bar) pour imprégner les fibres. Lorsque le moule est complètement rempli le moule est chauffé pour faire réticuler la résine. La pièce est finalement démoulée et peut éventuellement subir un traitement thermique post-cure pour améliorer la réticulation.

Equipement

- Moule
- Système d'ouverture/fermeture du moule (presse hydraulique pour les moules en acier, système de palans pour les moules en résine…)
- Machine d'injection

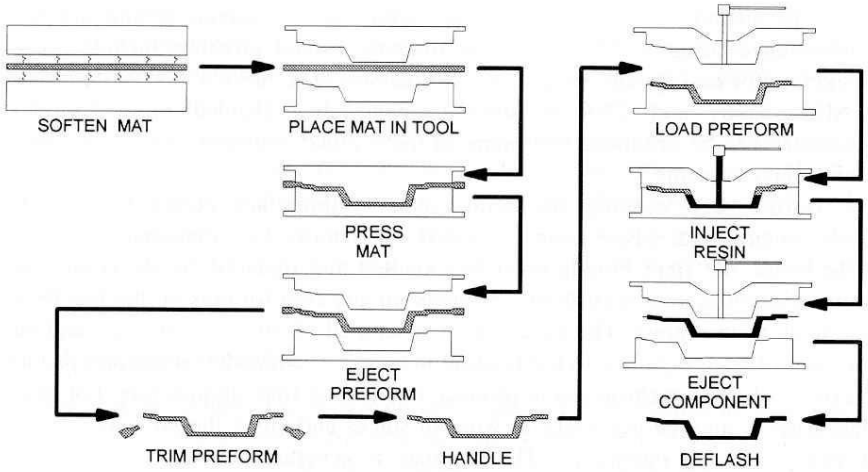

Figure 1: Resin transfer moulding (RTM)

Moule

Le moule est composé de deux moitiés et peut-être réalisé en différents matériaux selon la complexité et la quantité de pièces à produire.

Matériaux	Température maximum	Nombre de pièces maximum par moule	Prix
Polyester ou vinylester	~25°C	< 1000 pièces	Très bas
Epoxy	<60°C	< 4000 pièces	Bas
Nickel shell epoxy	<60°C	< 50'000 pièces	Assez bas
Aluminium	>60°C	< 20'000 pièces	Cher
Acier	>60°C	>20'000 pièces	Très cher

Tableau 1: Matériaux pour moule

Matériaux

Renfort fibreux

Quasiment n'importe quel type de fibres (par ex. verre, carbone, aramide, fibres naturelles….) sous n'importe quelle forme de renfort (par ex. mat, tissé, tressé, non-crimp…) peut être utilisé. Le renfort doit cependant être découpé au préalable à la forme du moule.

Dans le cas de pièces complexes tridimensionnelles, le drapage avec certains types de renforts (par ex. UD, non-crimp) peut devenir problématique. De même, les fibres courtes et les unidirectionnels sont plus rarement utilisés car ils risquent de bouger lors de l'injection de la résine.

Résine

- Les résines thermodurcissables sont principalement utilisées (des thermoplastiques qui polymérisent directement dans le renfort pendant l'injection tels qu'APLC12, Cyclics ou Elium font progressivement leur entrée sur le marché)
- Le temps de gel doit être suffisamment long pour remplir le moule complètement
- La viscosité de la résine doit être suffisamment basse pour imprégner rapidement le renfort fibreux

Inserts

Des cœurs pour des constructions sandwichs et des inserts métalliques peuvent être placés dans le moule avant injection.

Détails du procédé

Température

La température du moule est réglée en fonction du type de résine. Généralement la température la plus haute possible est préférée afin de diminuer la viscosité de la résine. Cependant, plus la température est haute plus la résine réticule rapidement et plus le temps de gel et la fenêtre de fabrication diminuent. Il faut donc trouver le meilleur compromis de température afin de remplir complètement le moule dans le minimum de temps.

Pression

Une pression d'injection de l'ordre de quelques bars est généralement choisie (jusqu'à 12bars). Une pression trop élevée risque de perturber le positionnement du renfort et donc les propriétés mécaniques de la pièce finale.

Points d'injection

En fonction de la taille et de la complexité de la pièce à réaliser il peut être nécessaire de prévoir plusieurs points d'injection et de vide. Une injection en ligne (runners) peut aussi être choisie. Le moule peut être rendu étanche avec des joints ou avec un "pinch-off edge" (figure2).

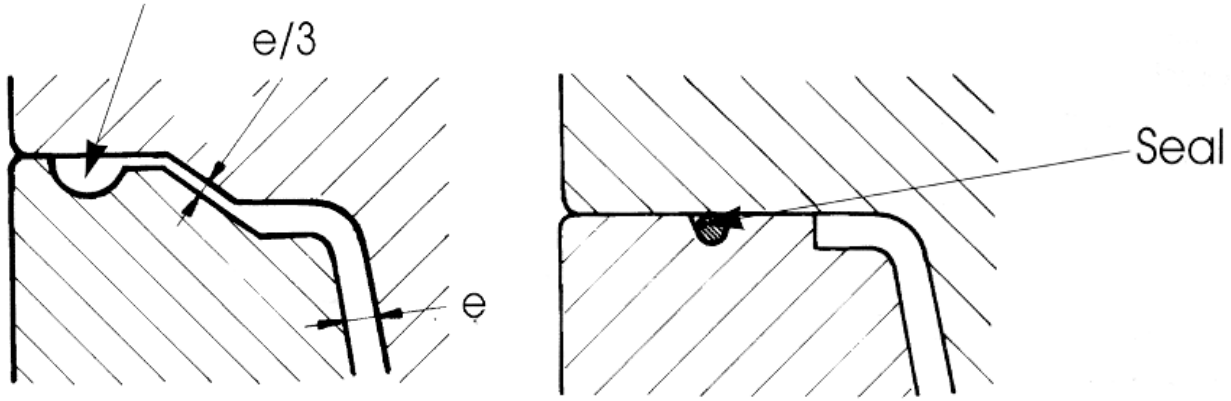

Figure 2: Pinch-off edge (gauche) et joint (droite)

Simulation

Pour garder un moule le plus simple possible tout en garantissant un remplissage rapide des simulations de remplissage sont possibles. Si le renfort est considéré comme un milieu poreux incompressible la loi de Darcy peut être utilisée pour calculer les vitesses d'imprégnation en fonction des paramètres des matériaux et du process. La loi de Darcy en 1-D est :

$$u = \frac{Q}{A} = -\frac{K}{\mu}\frac{\partial \mathrm{P}}{\partial \mathrm{x}}$$

Où u est la vitesse du fluide, Q le taux d'écoulement, A la section de la cavité, K la perméabilité du milieu poreux, μ la viscosité de la résine, $\frac{\partial \mathrm{P}}{\partial \mathrm{x}}$ le gradient de pression.

En 2-D (ce qui est le plus souvent le cas en RTM) la loi de Darcy s'écrit

$$\begin{pmatrix} u_x \\ u_y \end{pmatrix} = -\frac{1}{\mu}\begin{pmatrix} K_{xx} & K_{xy} \\ K_{yz} & K_{yy} \end{pmatrix}\begin{pmatrix} \partial \mathrm{P}/\ \partial \mathrm{x} \\ \partial \mathrm{P}/\ \partial \mathrm{y} \end{pmatrix}$$

La vitesse d'imprégnation est donc fonction de la viscosité de la résine, elle même fonction de la température. Le tenseur de perméabilité peut être modifié en choisissant différents matériaux ou combinaisons de matériaux. Si l'imprégnation est longue il devient nécessaire d'inclure la cinétique de réticulation de la résine dans l'équation.

Il existe plusieurs logiciels de simulation isotherme ou non-isotherme qui peuvent notamment prendre en compte le changement de viscosité dû à la réticulation de la résine. Les pièces de faible épaisseur peuvent être simulées en 2-D, les pièces plus épaisses avec des changements de

perméabilité dans l'épaisseur nécessitent en général une analyse 3-D. Examples de logiciels: PAM RTM, LIMS, VARTM-ISD and RTMFLOT.

Propriétés mécaniques

Le process RTM peut utiliser une large gamme de matériaux et de types de renforts et offre donc la possibilité d'obtenir une grande variété de propriétés mécaniques (Tableau 2). La RTM permet aussi de modifier localement le composite (type et nature des fibres) et est donc plutôt utilisée pour des pièces de structure.

	Vf (%)	**Résistance en flexion** (MPa)	**Module de flexion** (GPa)
Unidirectional	32-50	600-750	22-28
Tissé	32-45	300-400	15-21
Continuous glass preform	19-40	160-250	9-14
Continuous glass mat	7.5-25	65-180	5.5-11

Tableau 2: Examples de propriétés mécaniques (polyester-fibres de verre).

Il est plus facile de draper des renforts à fibres courtes dans des moules complexes mais les propriétés mécaniques seront inférieures comparées à des renforts à fibres continues. Le choix des matériaux sera dicté par le coût des matières premières, les performances souhaitées et les volumes de production.

Aspects économiques

Le critère le plus important dans la sélection d'une méthode de fabrication est presque toujours le coût ! (sauf pour les formules 1, satellites…).

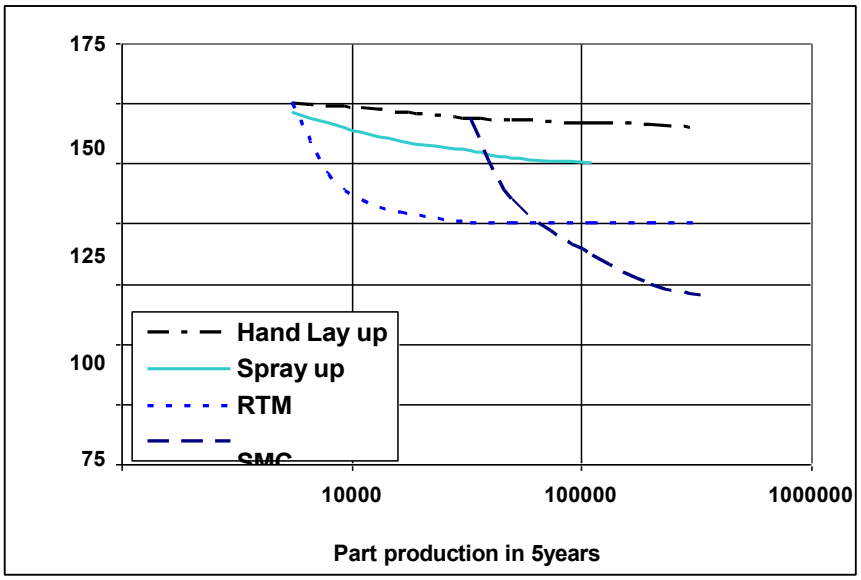

Figure 4: Comparaison schématique du coût de certains procédés

RTM comparé au moulage par compression

- Matériaux plus chers (textiles)
- Main d'oeuvre plus cher
- Moules et équipement beaucoup moins chers
- Meilleurs propriétés mécaniques
- Reproductibilité similaire
- Temps de cycle (beaucoup) plus longs

RTM comparé au moulage par contact et pas projection

- Moule plus cher
- Meilleurs propriétés mécaniques
- Meilleure reproductibilité
- Equipement plus cher
- Temps de cycle plus courts
- Main d'oeuvre moins cher
- Moins d'émission de composés volatiles

Figure 5: Toit de la BMW M3 (6000/an)

La RTM est récemment arrivée dans les productions à moyen volume du domaine automobile avec le toit de la BMW M3 (figure 5). Cependant il est dur pour ce procédé d'être compétitif avec l'acier à cause notamment de temps de cycle plus longs et de matériaux (tissé carbone) beaucoup plus chers même si le gain de poids est substantiel.

Applications

Le RTM permet de réaliser des pièces grandes et complexes. Grâce au choix des matériaux et du type de renfort ainsi que le type de process de fabrication il est possible d'adresser une large gamme d'applications.

Figure 6: Dodge Viper et coaue de voilier

Variantes du process RTM

Vacuum assisted Resin Transfer Moulding (VARTM)

En RTM standard l'air contenu dans le moule est chassé par la résine mais la plupart du temps on applique un vide de 0.5-0.7bar dans le moule (VARTM). Le vide nécessite un moule un peu plus complexe et un bon système de joints d'étanchéité, le moule est donc plus cher. Cependant le vide permet de réduire efficacement l'air et l'humidité contenus dans le moule et de diminuer la porosité de la pièce finale, les propriétés mécaniques s'en trouvent améliorées. L'application du vide augmente aussi le différentiel de pression et accélère le remplissage du moule.

Vacuum assisted Resin Infiltration (VARI, VART ou RTM Light)

Description

- Le renfort est placé dans le moule
- Un film, une membrane ou une coque flexible est utilisée pour fermer le moule et est tenue en place par un fort vide
- Le système d'injection est connecté au moule, on applique le vide au moule
- La résine imprègne le renfort
- Le vide est arrêté lorsque le moule est plein et la réticulation commence
- Après réticulation le moule est ouvert et la pièce démoulée

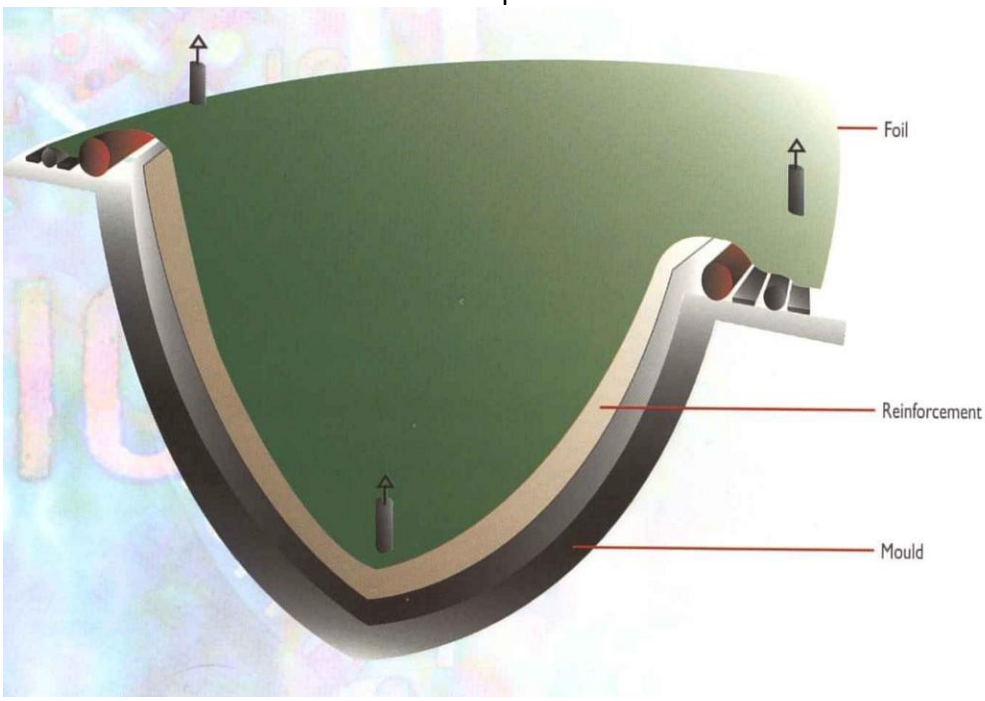

Figure 7: Procédé VARI

Equipement

- Double pompe à vide (fort vide pour fermer le moule, moyen pour imprégner le renfort)

Moule

- Le moule du bas est similaire à ceux utilisés en moulage par projection (Polyester, vinylester ou époxy)
- Plusieurs variantes existent pour le moule du haut :

Film à vide	**Membrane élastomère**	**Coque composite**
▪ Bon marché ▪ Undercuts possibles ▪ Qualité de surface moyenne ▪ Fermeture du moule assez longue ▪ Risque de déchirement ▪ Pas applicable pour des angles saillants ▪ Inspection visuelle possible ▪ Jetable	▪ Chère ▪ Undercuts possibles ▪ Qualité de surface correcte ▪ Facile à appliquer ▪ Risque de déchirement pendant le démoulage (absorbe les styrènes) ▪ Possible pour les angles pas trop saillants ▪ Réutilisabilité (100-200	▪ Plus chère ▪ Undercuts impossibles ▪ Bonne qualité de surface ▪ Facile à appliquer ▪ Facile à démouler ▪ Angles saillants possibles (R=5 mm) ▪ Meilleure distribution de la pression ▪ Meilleur contrôle de l'épaisseur

Comparé à la RTM

Comme il n'y a qu'une seule moitié de moule les forces de compaction atteintes sont moins importantes qu'en RTM et donc les fractions volumiques de fibres seront aussi moins élevées. Cependant les moules sont moins chers et cette technique peut être utilisée pour fabriquer de très grandes pièces (par ex. des coques de bateau). Les pièces sont souvent réticulées à l'ambiante.

SCRIMP RTM

Le procédé SCRIMP utilise un système breveté de distribution de la résine pour diminuer le temps d'infiltration nécessaire. Un textile à mailles très ouvertes est placé sur la surface du renfort. La résine se propage très rapidement dans ce textile et imprègne le renfort de façon transversale.

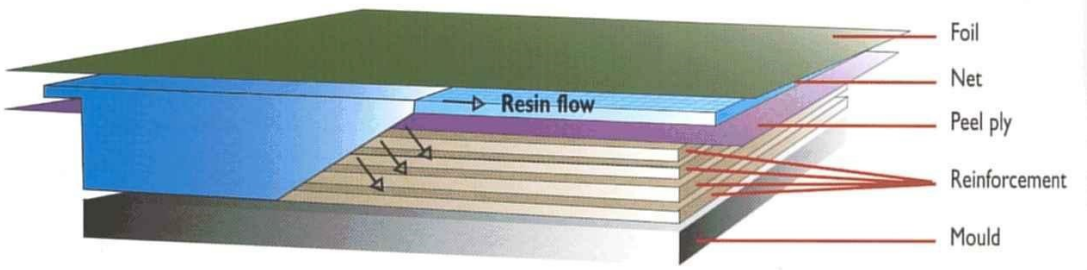

Figure 8: Procédé SCRIMP

Liquid injection Compression Moulding

Description

- La préforme est placé dans le moule
- Le moule est fermé mais pas jusqu'à l'épaisseur finale de la pièce (a).
- La résine est injectée dans le moule (b).
- Après injection le moule est fermé.
- La compaction due à la fermeture du moule améliore la distribution de la résine et l'imprégnation du renfort (c).

Equipement

Presse Hydraulique nécessaire (mais moins grosse qu'en SMC)

Moule

Acier et/ou alliages

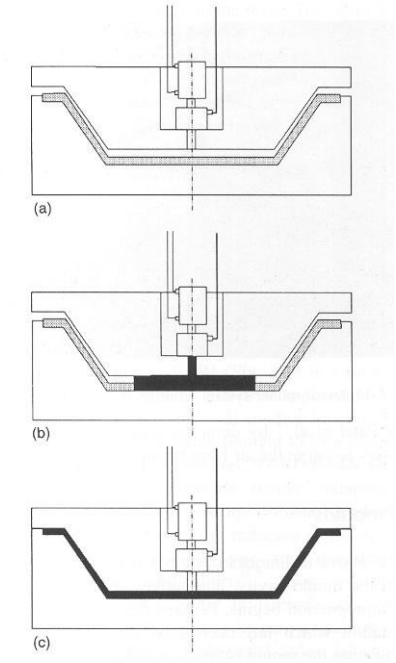

Figure 9: liquid injection-compression moulding.

Comparé avec la RTM

La presse hydraulique augmente considérablement le prix de l'équipement. De plus, des machines d'injection à haut débit sont nécessaires pour diminuer les temps de cycle requis pour des productions à haut volumes.

Les temps de cycles sont plus courts qu'en RTM (de quelques minutes à quelques secondes) grâce à l'injection plus rapide de la résine et des distances d'écoulement plus courtes qui de plus rendent possible l'utilisation de résines plus visqueuses. Cependant de l'air reste plus facilement bloqué dans le moule et les qualités de surfaces ne sont pas aussi bonnes qu'en RTM. Une couche de gelcoat est donc indispensable pour les pièces d'apparence. La porosité est aussi généralement plus élevée et les propriétés mécaniques un peu plus basses qu'en RTM.

References:

1.) S. Advani and E. M. Sozer, Lquid Moulding of Thermoset Composites, in Comprehensive composite materials, 2000.

2.) Johnson C.F. "Resin transfer moulding" Encyclopedia of polymer Science

3.) Rikart Gebart B. "Current issues in RTM", PPS conf. proc. Göteborg 1997

4.) Calhoun D.R. et al. "Mould filling analysis in RTM", Pol. comp., p.251, vol 17(2) 1996

Experimental Procedures to Run Longitudinal Injections to Measure Unsaturated Permeability of LCM Reinforcements ☆

Justin B. Alms**,b,2, Nuno Correia**,a,1, Suresh G. Advani**,b,2, Edu Ruiz*,c,3

[a] *Campus da FEUP, Rua Dr. Roberto Frias, 400 4200-465 Porto — Portugal*

[b] *Center for Composite Materials, 201 Composites Manufacturing Science Lab, University of Delaware, Newark, DE 19716-3144*

[c] *École Polytechnique of Montréal, Department of Mechanical Engineering, P.O. Box 6079, Station "Centre-Ville", Montreal, Canada, H3C 3A7*

Abstract

This standard is issued in order to create a set of experiments for one to characterize permeability of any given fabric used in a liquid composite molding process. This standard will establish a general procedure and list of experimental requirements to fulfill in order for your resulting permeability data to be considered valid by a general audience who is familiar with this field of work.

Key words: Permeability, Resin Transfer Molding (RTM), Resin Injection, One-D Flow Experiment

1. Scope

1.1.

This standard is designed to measure the permeabilities of unidirectional, woven, and stitched preform fabrics. This standard is only designed to be used to measure the in-plane (parallel to woven plane) directions.

1.2.

This standard uses a mold with two rigid molding surfaces commonly used in the Resin Transfer Molding (RTM) process. Performing the experimental procedure described within this standard characterizes the fabric permeability at one fiber volume fraction. To characterize the permeability as a function of fiber volume fraction, this procedure must be conducted at least three times while varying the fiber volume fraction (i.e. varying the number of layers or mold thickness).

1.3.

Over the years, many permeability characterization methods to experimentally measure permeability have been developed. Richard Parnas in 1995 while leading the Polymer Composites division at the National Institute of Standards and Technology was the first to suggest such a standard [1, 2]. Since then many experimental characterization techniques have been developed in Trochu and Advani research groups for single scale and dual scale fabrics [3–8]. There are other researchers who have also reported characterization and measurement techniques with different modifications. This standard does not plan to address all concerns and possible permeability char-

☆This document is a collaborative effort among members of the FPCM international conference series.

*Principle Corresponding author

**Corresponding author

Email addresses: jbalms@udel.edu (Justin B. Alms), ncorreia@inegi.up.pt (Nuno Correia), advani@udel.edu (Suresh G. Advani), edu.ruiz@polymtl.ca (Edu Ruiz)

[1] Institute of Mechanical Engineering and Industrial Management

[2] Center for Composite Materials, University of Delaware

[3] Center for Applied Research on Polymers and Composites, École Polytechnique Montréal

acterization methods but will focus on providing guidelines for interested researchers to follow a test method for specific fabrics. The results of which will be compiled and reliability of the test method evaluated as a publication with all the participating researchers as co-authors.

2. Terminology: Symbols

A_W = Aerial weight, weight of one layer of reinforcement per unit area, [g/m^2];
CV = Permeability coefficient of variation, [%];
$\boldsymbol{\epsilon}$ = Percentage error, [%];
h = Thickness of the fabric stack, [m];
I = Pressure integral value, [Pa·s];
K_{exp} = Experimental permeability in the length direction of the mold, [m^2];
$\bar{K}_{exp}$ = Average of experimentally measured permeability, [m^2];
K^0_{exp} = Measured permeability in the warp direction, [m^2];
K^{45}_{exp} = Measured permeability at 45°, [m^2];
K^{90}_{exp} = Measured permeability in the weft direction, [m^2];
L = Length of the fabric, [m];
m = Slope of $x_{ff,i}$ vs. t_i trendline, [m^2/s];
M_f = Mass of all fabric layers used in an experiment, [g];
μ = Viscosity of fluid, [Pa·s];
n = Number of (x_{ff}, t) data points recorded in an experiment;
N = Number of experiments in a set;
N_L = Number of fabric layers.
ϕ = Porosity of fabric, (1-V_f);
P_I = Injection pressure at the inlet, driving the fluid flow, [Pa];
$\bar{R}$ = Average of racetrack factor;
ρ_f = Density of the reinforcement, [g/m^3];
s_{n-1} = Permeability standard deviation, [m^2];
t = Time during infusion, [s];
V_f = Fiber volume fraction, (1-ϕ);
W = Width of the fabric, [m];
x_{ff} = Fluid flow front, [m];
x_f = Farthest flow front position from inlet, [m];
x_n = Nearest flow front position from inlet, [m]; and

3. Summary of Test Method

In this test, several layers of a fabric preform used for making Fiber Reinforced Plastics (FRP) are cut into rectangles and stacked into a rigid mold. The fabric stack is then compressed by closing the mold, bringing the two surfaces of the mold together until they come in contact with the rigid spacer frame forming an air tight seal. Once the mold is closed and secured, a liquid resin or test fluid is injected into the mold cavity. The fluid flows through the open pores or free spaces within the fibrous reinforcement. The resin is injected into the mold in a manner in which results in a one dimensional flow front pattern. As the flow progresses the fluid flow front is recorded at several times throughout the injection. The injection is discontinued once the resin flow front reaches the vent side of the mold. An analysis based on Darcy's Law (1) [9] is then conducted to

$$\langle \mathbf{u} \rangle = \frac{\mathbf{K}}{\mu} \cdot \frac{\partial P}{\partial \mathbf{x}} \tag{1}$$

determine the permeability in the direction parallel to the resin flow [10, 11]. In Equation (1) $\langle \mathbf{u} \rangle$ represented the volume average flow velocity, $\mathbf{K}$ is the permeability tensor, and $\partial P/\partial \mathbf{x}$ is the pressure gradient.

4. Experimental Materials

4.1. Fabric

The fabric preform used in the permeability experiments which follow this standard should have a similar architecture to typical fiber used in FRPs. These fabrics should have a regular structural pattern with a high degree of uniformity throughout the entire supply of fabric which is used in a set of experiments. Only a single material should be used in a given set of experiments.

This procedure and analysis does not claim to provide any information on permeability of a laminate of multiple types of fabric.

4.1.1. Fabric Layer Dimensions

Though mold dimensions should not have an effect on permeability, certain conditions should be met to minimize effects which commonly occur and cause invalid permeability results. In order to minimize the influence of non-uniform nesting between experiments, the number of layers placed into the mold is prescribed to be 10. The compressed fabric stack-up should have a thickness between 2.5 and 10.0mm (thickness of the spacer plate) and should be longer than it is wide. The length of the fabric is defined in the direction of the resin flow. The aspect ratio η, defined in (2), should adhere to the following condition also shown in (2):

$$\eta = \frac{length}{width} \geq 3.0 \tag{2}$$

4.2. Fluid

Thermosetting polymeric resins are the typical fluid used in the actual manufacturing of the FRPs. These fluids are normally assumed to be Newtonian, at least prior to gelation, and as such only a Newtonian fluid should be used as a test fluid for experimentation. Also the fluid should have uniform properties, thus fluids with suspended particles or catalyzed resins should not be used in conjunction with this measurement technique. As standard test fluid, silicone oil of controlled properties is preferred for experimentation. The uniformity of the fluid should be verified by measuring the viscosity of the fluid before and after it has infused the fabric. Lastly, the fluid should have a comparable viscosity to typical resin systems used in the Liquid Composite Molding (LCM) manufacturing industry. The viscosity, μ, of the fluid should fall within the range given in (3):

$$100.0 \leq \mu \leq 200.0 centipoise \tag{3}$$

5. Apparatus

5.1. Mold Assembly

A proper mold must be used in order for the characterization of one dimensional permeability. A typical characterization mold is composed of five key components, one top molding surface, one bottom molding surface, one intermediate frame (spacer plate), one injection connection, and one venting connection. A schematic representation of a typical mold is shown in Figure 1. Other mold configurations are also possible while respecting

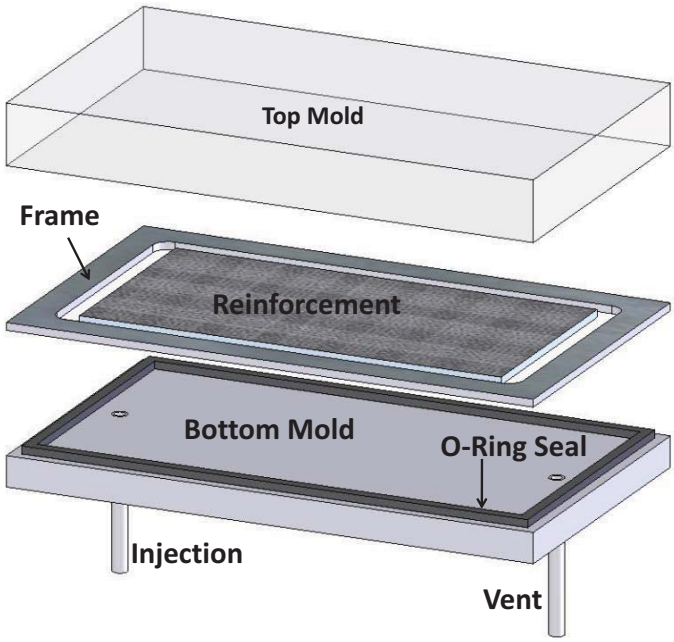

Figure 1. Schematic representation of a typical mold to be used in conjunction with this standard.

the guidelines of Sections 5.1.1 to 5.1.3. Additional necessary hardware not shown in Figure 1 includes a positive pressure chamber such as a spray paint pressure pot and a calibrated pressure sensor.

5.1.1. The Mold Surfaces

Both top and bottom molding surfaces must be specifically designed to resist deflection as much as possible during the closing of the mold which compresses the fabric. Special care must be taken to reduce the deflection as much as possible. The amount of deflection should be approximated using a standard analytical technique such as plate theory, a numerical technique, or directly measured using an experimental technique. A description of these efforts and results of calculating this approximation are to be included in the report-

ing requirement along with measured permeability values.

Minimizing deflection is important because permeability analysis technique for analyzing one dimensional flow using Darcy's Law (1) [9] assumes a constant thickness throughout the length and width of the mold. The acceptable limit of mold deflection is defined as 2% of the nominal thickness of the mold.

5.1.2. The Intermediate Frame

The intermediate frame also known as the spacer plate goes between the two molding surfaces and defines the thickness and thus fiber volume fraction of the laminate to be infused. The frame also defines the inner cavity in which fabric preform layers will be placed. It is important to cut the fabric layers carefully to exactly fit within this cavity so that the fabric edges come directly into contact with the frame walls. The only important measurement for the frame is that it should have a uniform thickness and should conform to at least an ISO IT10 geometric tolerance. Several measurements should be taken using accurate calipers of the frame and the details of these measurements will be included in the reporting requirements.

5.1.3. The Inlet and Vent Tubes

The inlet and vent tubes should have a secure connection to the bottom mold surface. Prior to the injection of resin or test fluid the inlet and vent tubes should be in fluid contact with an empty space which allows resin flow along the entire width of the mold to ensure one dimensional flow. Shown in Figure 2 is a schematic illustration of a typically tube, empty gap, fabric, silicone seals, and frame arrangement.

5.1.4. The Fluid Injection System

The injection unit is a container in the form of a pressure pot in which the resin or test fluid can be deposited prior to injection. This container is then tightly closed and pressurized. The container should be free of air leaks at the prescribed injection pressure. Also the air pressure inside of the container should be controlled by a pressure

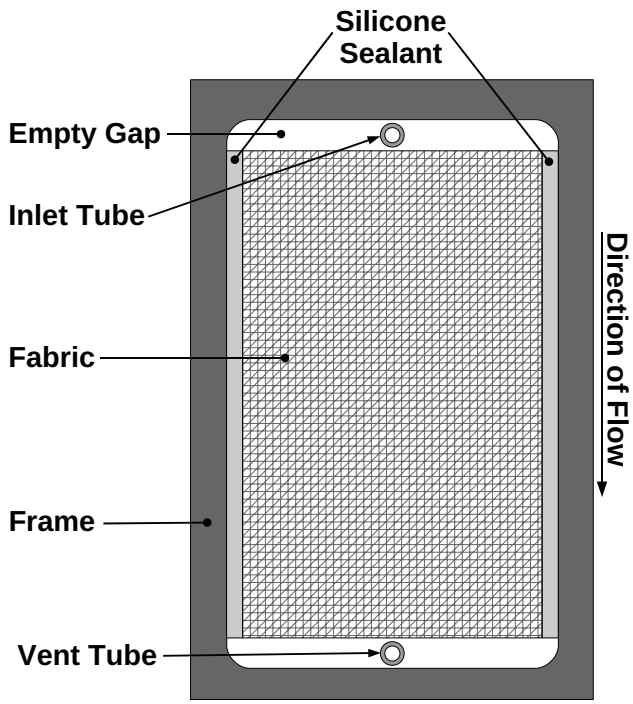

Figure 2. Top view schematic representation of a typical arrangement of the inlet and vent tubes, fabric, frame, empty gap, and silicone seals.

regulator. Pressure must be kept constant during injection with a deviation of no more than 2% of nominal injection pressure.

5.1.5. The Pressure Sensor

A calibrated pressure sensor should be placed in fluid contact with the empty gap connected to the resin inlet. The pressure sensor is intended to produce the best possible data for the injection pressure independent of various hardware configurations. The pressure transducer should be located near the entry point to the mold in such a way that hydrostatic pressure is measured. This is usually done by placing the pressure sensor on a "T" fixture, where the transducer is opposed to the fluid inlet. The pressure transducer should have a manufacturer's accuracy rating of 0.5% Full Scale (FS) or lower.

5.1.6. Data Acquisition Unit

A data acquisition unit is required to record the injection pressure in real time during the experiment. The unit needs also to acquire the position of the fluid flow front during the injection.

The technique used to track the flow front evolution has to be accurate enough to detect not only its position but also any flow distortion such as edge effects (also known as race-tracking) which are an important source of error.

6. Procedure

6.1. Measure Fabric Compressibility

To facilitate an accurate approximation of mold deflection the first step is to characterize the fabric preform compressibility. Flat plates should be mounted to both fixtures of an instron machine. A minimum of $15mm$ of uncompressed fabric layers are stacked on the bottom fixture. The fabric is compressed at a cross head rate of 1 millimeter per minute. During the compression the force on the load cell and displacement of the cross head are constantly recorded. Knowing the force, area of the fabric layers, and the displacement of the cross head; a correlation should be created for this tested fabric between pressure, thickness, and fiber volume fraction.

6.1.1. Exceptions

The process of measuring fabric compressibility may be omitted if any of the following conditions are met:

1. If the mold closure is accomplished by placing the entire mold inside an industrial style hydraulic press with adequately thick platens to reinforce the mold.
2. If the mold deflection is experimentally measured to ensure it is below the acceptable limit.

6.2. Fabric Cutting

The fabric can be cut by hand with an appropriate template or preferably with an automated fabric cutting machine. Special care should be used to make sure that the all cuts are either parallel or perpendicular to principal in-plane tow directions of the fabric. The most important aspect of the fabric cutting is the dimensional tolerance, δ, of width of the cut fabric shown in (4).

$$\delta = \begin{matrix} +1.0mm \\ -0.0mm \end{matrix} \tag{4}$$

This tolerance is specified to prevent the formation of racetracking which occurs when the fabric width is smaller than the inner width of the mold frame. The width of fabric should be cut as close as possible to fit exactly into the mold frame.

6.3. Fabric Mass Measurement

After the layers of fabric have been cut, stack the fabric on top of each other. Using an accurate and calibrated scale with a resolution of at least $0.1g$, measure the mass of the fabric stack. Record this measurement as it will later be used to calculate the fiber volume fraction.

6.4. Mold Assembly

First the inlet and vent tubes are connected to the bottom molding surface. The tube connections should be made to be air tight. The frame is than placed on top of the bottom surface. The interaction of the frame and the molding surface must have a sealing gasket to prevent any fluid leakage during the injection. Then the fabric preform layers are stacked on top of the bottom molding surface and in between the walls of the frame as shown in Figures 1 and 2, the number of layers shall be prescribed to 10. To avoid any racetracking of the resin to take effect, a silicone sealant can be used on the sides of the preform (see detail on Figure 2). The upper half of the mold is then placed on top of the fabric and frame.

6.4.1. Component Alignment

During the stack up of these components alignment during placement is critical to prevent the fabric layers from becoming moved during mold assembly. A typical effort to providing sufficient alignment is to have holes drilled through all the components in the four corners of the mold. Metallic pins can be inserted into these holes prior placement of the frame, fabric, and top molding surface.

6.5. Mold Closure

The mold is closed by compressing the fabric until both molding surfaces become into contact with the frame. Mold closure can be accomplished by perimeter bolting, perimeter clamping, or by

placing the entire mold into a device similar to a hydraulic press. If a perimeter closing technique is used the maximum deflection of the middle of the mold should be calculated, and additional reinforcing methods are recommended.

6.6. Resin Injection

6.6.1. Measure Fluid Viscosity

A resin or test fluid should be prepared and the fluid viscosity should be measured with a calibrated viscometer or rheometer. The viscosity measurement should be conducted at the same temperature at which the resin or test fluid will be injected.

6.6.2. Pressurize the Fluid

Once the fluid viscosity is known it is placed inside of the pressure pot and the pressure pot is closed to form an air tight seal. A tube is arranged so that once the pot has been pressurized the resin will come out of the pressure pot. At this point this tube should be clamped or closed in any other manner to prevent resin flow. A compressed air source is attached to an air pressure regulator which feeds the pressure pot. The injection pressure, P_{INJ}, of the fluid must be sufficiently large so that the dominating driving pressure of the fluid is the applied pressure and not capillary pressure. Injection pressure should not be too high to avoid any fiber washout or significant mold deflection. The limits on injection pressure are shown in (5).

$$100kPa \leq P_I \leq 200kPa \tag{5}$$

6.6.3. Initiate Fluid Flow

Prior to injection, the data recording system in place should be turned on. The pressure at the inlet should be recorded during the injection as well as the time and flow front position. The inlet tube is then opened to allow fluid flow through the mold. Once resin begins to flow out of the vent tube, the data acquisition system may be discontinued. The inlet tube remains open until an amount of resin suitable for a viscosity measurement flows through the vent tube into a container. Once the appropriate amount of resin has been collected the inlet tube may be closed.

6.6.4. Measure Final Fluid Viscosity

To verify the fluid used in the experiment was uniform during the injection the viscosity of the fluid which exits the mold must be measured. The process of collecting fluid which has infused the fabric and measuring its viscosity is only required once for a given set of permeability experiments given that the same batch of fluid is used throughout all the experiments in the set.

7. Number of Experiments

7.1. In-Plane Isotropic Materials

For materials which are isotropic in the plane such as Continuous Filament Mat (CFM) a minimum of three experiments should be conducted.

7.2. In-Plane Anisotropic Materials

For materials with different warp and weft permeabilities, such as unidirectional, woven, or stitched fabrics, at least three sets of experiments must be conducted. One set is conducted in the warp direction, 0°, another set is in the weft direction, 90°, and the last set is in between the warp and weft directions, 45°. Each set consist of at least three identical experiments for the purpose of statistical averaging.

8. Calculations

Two techniques can be used to perform the calculation of the unidirectional permeability measured through this standard. The first case is based on a linear interpolation of the squared flow front position in time while the second case uses an statistical approximation of the experimental data. Both techniques should result in similar values. The two techniques are detailed in Sections 8.2 and 8.3.

8.1. Fiber Volume Fraction

Fiber volume fraction, V_f, is a measure which represents the percentage of volume in the mold which is occupied by the reinforcement. Since the permeability of a material is a function of V_f it is important to report this value along with the permeability measurements. For each experiment

calculate the V_f and include it in the report. To calculate V_f, first calculate the aerial weight of the fabric as follows:

$$A_W = \frac{M_f}{L\,W\,N_L} \tag{6}$$

Then calculate the V_f as follows:

$$V_f = \frac{A_W\,N_L}{\rho_f\,h} \tag{7}$$

Lastly, porosity, ϕ, is a measure related to V_f which represents the volume percentage of empty space in the mold and is calculated as follows:

$$\phi = 1 - V_f \tag{8}$$

8.2. Squared Flow Front Approach

In order to determine the one dimensional permeability for a constant injection pressure test, the experimental flow front position must be plotted versus time. This graph should look similar to the one on Figure 3.

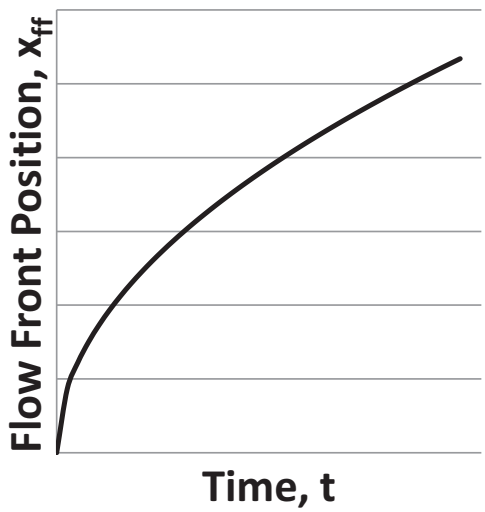

Figure 3. Schematic graph of typical constant pressure flow front position versus time results.

The flow front position must then be squared and plotted versus time. According to Darcy's law, this should look as a straight line as depicted in Figure 4. A linear trend line can then be obtained from this treated data. The slope of this trend line, m, is then determined for the characterization of permeability. For a one-dimensional

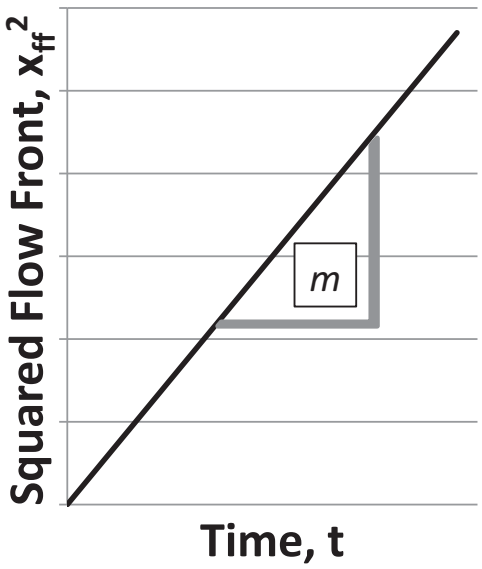

Figure 4. Schematic graph of typical constant pressure flow front position squared versus time results. This line is normally produced by computing a linear trend line of the recorded data points. The slope of this line is the shown parameter, m.

constant pressure injection, the permeability of the fibrous reinforcement can be evaluated based on Darcy's law as shown in (9).

$$K_{exp} = \frac{x_{ff,i}^2\,\phi\,\mu}{2\,P_I\,t_i} \tag{9}$$

Using Equation (9) and the slope, m, of the graph shown in Figure 4, the experimental permeability value can be obtained as follows (10).

$$K_{exp} = \frac{\phi\,\mu}{2\,P_I}\,m \tag{10}$$

The error of the measure using this analysis technique can be estimated in the following form:

$$\boldsymbol{\epsilon} = 100 \times \sqrt{\frac{1}{n}\sum_{i=1}^{n}\left(x_{ff,i} - \sqrt{m\,t_i}\right)^2} \tag{11}$$

8.3. Least Square Fit Approach

A least square fit can be applied to the experimental pressure data in order to estimate permeability value that will be self-correlated to Darcy's law. The integral solution of a Darcy's flow can

be computed in the following form (12) and (13) [3].

$$I(t) = \int_0^t P_I(t)dt \cdots$$

$$= \sum_{i=2}^{n} \left[\left(\frac{P_{I,i-1} + P_{I,i}}{2} \right) (t_i - t_{i-1}) \right] \quad (12)$$

$$x_{ff} = \left(\frac{2\,K}{\mu\,\phi}\, I(t) \right)^{1/2} \quad (13)$$

By applying a least square fit on equation (13), the following parameter a can be calculated using equation (14) and (15).

$$a = \frac{\sum_{i=2}^{n} x_{ff,i} \sqrt{I_i}}{\sum_{i=2}^{n} I_i} \quad (14)$$

$$I_i = \left(\frac{P_{I,i-1} + P_{I,i}}{2} \right) (t_i - t_{i-1}) \quad (15)$$

The value of parameter a calculated using equation (14) finally leads to the mean permeability value as follows (16).

$$K_{exp} = \frac{a^2\,\mu\,\phi}{2} \quad (16)$$

The error of the measure using this analysis technique can be estimated in the following form:

$$\epsilon = 100 \times \sqrt{\frac{1}{n-1} \sum_{i=2}^{n} \left(x_{ff,i} - a\sqrt{I_i} \right)^2} \quad (17)$$

8.4. Racetracking

Racetracking is the fluid flow behavior which occurs when there is a specific area of relatively low resistance to flow. This most often occurs along the edges of the mold where the fabric contacts the inner walls of the intermediate frame. This behavior has an effect on the apparent one dimensional permeability and it is nearly impossible to prevent completely [12]. For each experiment calculate the average racetrack factor in (18) and include it in the report.

$$\bar{R} = \left(\sum_{i=1}^{n} x_{f,i} - x_{n,i} \right) / (n \cdot L) \quad (18)$$

8.5. Statistics

For each set of permeability experiments, calculate the average permeability, standard deviation, and coefficient of variation as follows:

$$\bar{K}_{exp} = \left(\sum_{i=1}^{N} K_{exp,i} \right) / N \quad (19)$$

$$s_{n-1} = \sqrt{\frac{\left(\sum_{i=1}^{N} K_{exp,i}^2 - N\left(\bar{K}_{exp}^2\right) \right)}{(N-1)}} \quad (20)$$

$$CV = 100 \times s_{n-1} / \bar{K}_{exp} \quad (21)$$

8.6. Permeability Tensor

The square root of the effective permeability along one direction of a porous medium, K_{exp}, follows an ellipse as displayed in Figure 5, where the semi-major and minor axes [4] represent the

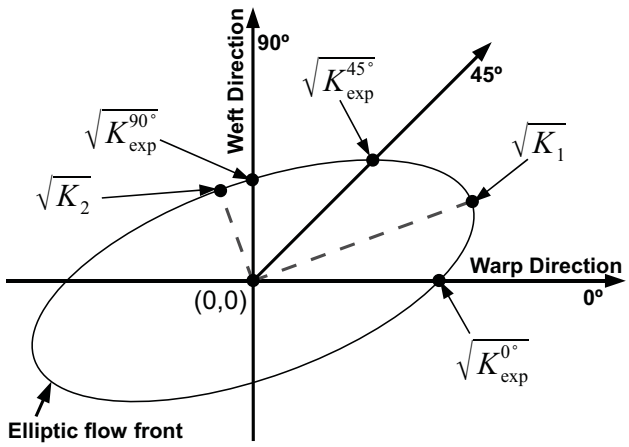

Figure 5. Elliptic pattern of the in-plane permeability tensor showing the effective permeabilities.

square roots of the principal permeabilities, K_1 and K_2. The principal values of the permeability tensor K_1 and K_2 can be estimated by measuring the permeability of the fibrous reinforcement K_{exp} at three different directions. In order to evaluate the permeability tensor of a reinforcement, three sets of permeability measures need to be carried out following this standard. These measures have to be conducted at different directions on the fibrous reinforcement, at warp (0°), weft (90°) and at 45° as depicted on Figure 6. From

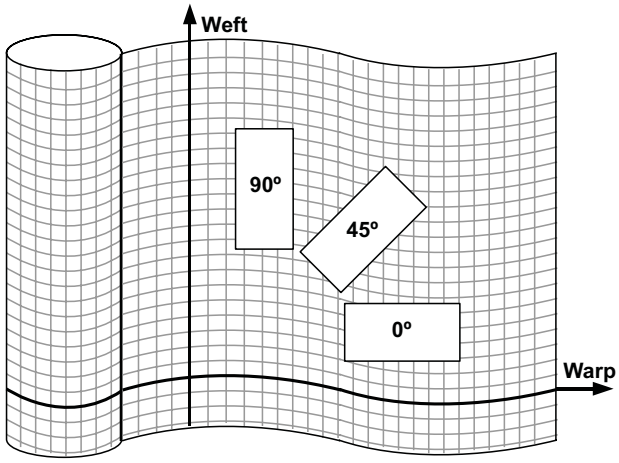

Figure 6. Sketch for cutting out the samples from the bulk roll to measure permeability of unbalanced fibrous reinforcements.

the effective permeabilities measured on each direction, the principal permeabilities can be computed following (22-26) [5, 13].

$$K_1 = K^0_{exp} \frac{(\alpha - \gamma)}{\left(\alpha - \frac{\gamma}{\cos(2\beta)}\right)} \tag{22}$$

$$K_2 = K^{90}_{exp} \frac{(\alpha + \gamma)}{\left(\alpha + \frac{\gamma}{\cos(2\beta)}\right)} \tag{23}$$

$$\beta = \frac{1}{2} tan^{-1}\left(\frac{\alpha}{\gamma} - \frac{\alpha^2 - \gamma^2}{K^{45}_{exp}\gamma}\right) \tag{24}$$

$$\alpha = (K^0_{exp} + K^{90}_{exp})/2 \tag{25}$$

$$\gamma = (K^0_{exp} - K^{90}_{exp})/2 \tag{26}$$

9. Report

The report of any experiment set should include all the following information. All variation from this procedure should also be reported to form a basis for the results.

1. Complete description of the fabric material used:
   - Type of material.
   - Description of the weaving pattern.
   - Description of fiber sizing (if known).
2. Complete description of the test fluid used including:
   - Composition of the fluid.
   - Any preparation procedure of the test fluid.
   - Viscosity measurement of the test fluid before each injection.
   - Viscosity measurement before and after at least one injection in each set of experiments.
   - Temperature of the test fluid before each infusion.
3. Details of the cutting procedure.
4. Fiber volume fraction of each experiment according to Section 8.1.
5. Results of each measure according to Sections 8.2 or 8.3, including the experimental error described in these sections.
6. The race-tracking factor for each experiment, as given by Equation (18) in Section 8.4.
7. All statistical parameter identified in Section 8.5.
8. The number of experiments conducted.
9. Experimental Conditions:
   - The date and location of each experiment.
   - The temperature of the testing laboratory during each experiment.
   - Temperature of the mold during each experiment.
10. Complete description of the test apparatus.
   - Mold Dimensions
   - Average and standard deviation of mold frame thickness measurements.
   - Approximate mold deflection or description of efforts used to prevent deflection.
   - Description of the flow detection subsystem such as sensors or video.
   - Best approximation of measurement sensitivity of flow detection system.

11. The components of the permeability tensor, K_1 and K_2, as described in Section 8.6.
12. Complete description of any variation to test procedure.

10. Acknowledgements

The authors wish to thank Onera - The French Aerospace Lab and Katholieke Universiteit Leuven, the organizers of the Permeability Benchmark Group (`http://permeability.onera.fr/`), Hexcel for providing the reinforcement, and all the participants of the permeability benchmark exercise.

References

[1] Richard S. Parnas, J. Grant Howard, Thomas L. Luce, and Suresh G. Advani. Permeability Characterization: Part 1: A Proposed Standard Reference Material. *Polymer Composites*, 16(6):429–445, DEC 1995.

[2] Richard S. Parnas, J. Grant Howard, Thomas L. Luce, and Suresh G. Advani. Permeability Characterization: Part 2: Flow Behavior in Multiple-Layer Preforms. *Polymer Composites*, 16(6):446–458, DEC 1995.

[3] Pierre Ferland, Dominique Guittard, and François Trochu. Concurrent Methods for Permeability Measurement in Resin Transfer Molding. *Polymer Composites*, 17(1):149–158, FEB 1996.

[4] J. R. Weitzenböck, R. A. Shenoi, and P. A. Wilson. Measurement of Principal Permeability with the Channel Flow Experiment. *Polymer Composites*, 20 (2):321–335, 1999.

[5] C. Demaria, Edu Ruiz, and François Trochu. In-plane Anisotropic Permeability Characterization of Deformed Woven Fabrics by Unidirectional Injections. Part I: Experimental Results. *Polymer Composites*, 28(6):797–811, DEC 2007.

[6] Pavel B. Nedanov and Suresh G. Advani. A Method to Determine 3D Permeability of Fibrous Reinforcements. *Journal of Composite Materials*, 36(2):241–254, 2002.

[7] J. Slade, E. Murat Sozer, and Suresh G. Advani. Effect of Shear Deformation on Permeability of Fiber Preforms. *Journal of Reinforced Plastics and Composites*, 19(7):552–568, MAY 2000.

[8] Nina Kuentzer, Pavel Šimáček, Suresh G. Advani, and Shawn Walsh. Permeability Characterization of Dual Scale Fibrous Porous Media. *Composites Part A: Applied Science and Manufacturing*, 37(11):2057–2068, 2006.

[9] Henry Darcy. *Les fontaines publiques de la Ville de Dijon*. Libraire des Corps Imperiaux des Ponts et Chausses et des Mines, Paris, 1856. Editor: Victor Dalmont.

[10] R. Gauvin and M. Chibani. The Modeling of Mold Filling in Resin Transfer Molding. *International Polymer Processing*, 1(1):42–46, 1986.

[11] Suresh G. Advani and E. Murat Sozer. *Process Modeling in Composite Manufacturing*. Marcel Dekker, Inc., 270 Madison Ave., New York, NY 10016, 2002.

[12] Jeffrey M. Lawrence, John Barr, Rajat Karmakar, and Suresh G. Advani. Characterization of Preform Permeability in the Presence of Race Tracking. *Composites Part A: Applied Science and Manufacturing*, 35(12):1393–1405, 2004.

[13] C. Demaria, Edu Ruiz, and François Trochu. In-plane Anisotropic Permeability Characterization of Deformed Woven Fabrics by Unidirectional Injections. Part II: Prediction Model and Numerical Simulations. *Polymer Composites*, 28(6):812–827, DEC 2007.

14
Permeability properties of reinforcements in composites

V. MICHAUD, Ecole Polytechnique Fédérale de Lausanne (EPFL), Switzerland

Copyrighted Material downloaded from Woodhead Publishing Online
Delivered by http://www.woodheadpublishingonline.com
EPFL Lausanne (569-11-299)
Sunday, January 29, 2012 6:21:28 AM
IP Address: 128.178.195.215

Abstract: Permeability is defined from the equations of fluid flow through porous media. Modelling of the saturated permeability tensor is then presented using a historical perspective, going from the first geometrical models developed in soil science, to recent unit-cell models based on a precise description of composite reinforcements. Deviations from the saturated flow models are then presented, discussing in particular the effect of capillarity. Finally, experimental methods to measure permeability are described and discussed.

Key words: permeability, saturation, Darcy's law, liquid composite moulding, textiles.

14.1 Introduction

Reinforcements used in the production of polymer composite materials are in general thin filaments or fibres, assembled into yarns or tows, which are further assembled into a fabric. This initially dry fibre assembly thus constitutes a self-sustaining porous body or 'preform'. During composite processing, a fluid precursor of the matrix phase (a thermoset resin, a thermoplastic polymer or pre-polymer) is made to infiltrate the open pore space within the preform. Upon subsequent chemical reaction or solidification of the matrix precursor, a composite material is produced. The drive to manufacture sound and homogeneous parts at the lowest cost has driven the need to predict the kinetics of the process, as well as the local void and fibre content distribution within the composite, and in some cases residual strain or stress fields that may have built up in the final part. All these final attributes of the process and the resulting part are influenced by the flow characteristics of the fluid matrix precursor into the preform, which are chiefly governed by the fluid viscosity and the resistance to flow brought by the reinforcement. This last point is generally expressed by the permeability of the preform, the object of the present chapter. We will first describe porous media constituted by the more common composite reinforcement preforms, and then define their permeability as it emerges from the equations of flow through porous media. Modelling of the saturated permeability tensor will be presented

© Woodhead Publishing Limited, 2011

from a historical perspective, starting with the first geometrical models developed in soil science, and then moving to more recent unit-cell models that couple precise descriptions of the fluid flow path with realistic models of the reinforcement phase used in producing the composite. Deviations from such saturated models arise, however, when the fluid does not fill all open pore space within the preform: fluid flow is then said to be unsaturated, and the problem is then one of multiphase flow. Experimental methods used in the measurement of permeability are then described, and discussed by comparison with theoretical models.

14.2 The permeability tensor

14.2.1 Porous medium description

Textile reinforcements used in composite processing have been described in detail in the previous chapters of this book, together with strategies used in modelling their internal geometry. The mechanical behaviour of dry textile reinforcement has also been described in several chapters: it is important to note that composite reinforcements tend to deform and shear rather easily, with a frequently hysteretic behaviour.

For the purpose of the present chapter, the fabrics or preforms are considered as porous media to be invaded or 'infiltrated' by a fluid phase. Many methods to describe such preforms can be found in other branches of engineering dealing with porous media, such as soil science, reservoir engineering, textile engineering and membrane science (Bear, 1972; Dullien, 1979; Scheidegger, 1974). Like most porous media, reinforcements used in composite processing are statistical by nature, so a complete description of their pores would require mapping the internal geometry of the whole preform, a task that is still beyond reach in practical cases. A continuum mechanics approach, calling for average properties of the reinforcement, is thus used in most models. This rests on the definition of a representative volume element (REV), large enough to contain representative averages of all phases, solid, liquid and gas, yet small enough to be considered as a differential element on the scale of the preform, to which the model assigns only average values of relevant process parameters such as temperature or pressure. Figure 14.1a provides an example of REV for a reinforcement fabric, and Fig. 14.1b shows a typical micrograph, for a non-crimp fabric composite which was incompletely infiltrated, showing tows, matrix and porosity. A REV contains in the most general case what remains of the initial atmosphere, the fibres, and infiltrated liquid, in respective volume fractions V_a, V_f and V_l, such that

$$V_a + V_f + V_l = 1 \qquad 14.1$$

Copyrighted Material downloaded from Woodhead Publishing Online
Delivered by http://www.woodheadpublishingonline.com
EPFL Lausanne (569-11-299)
Sunday, January 29, 2012 6:21:28 AM
IP Address: 128.178.195.215

© Woodhead Publishing Limited, 2011

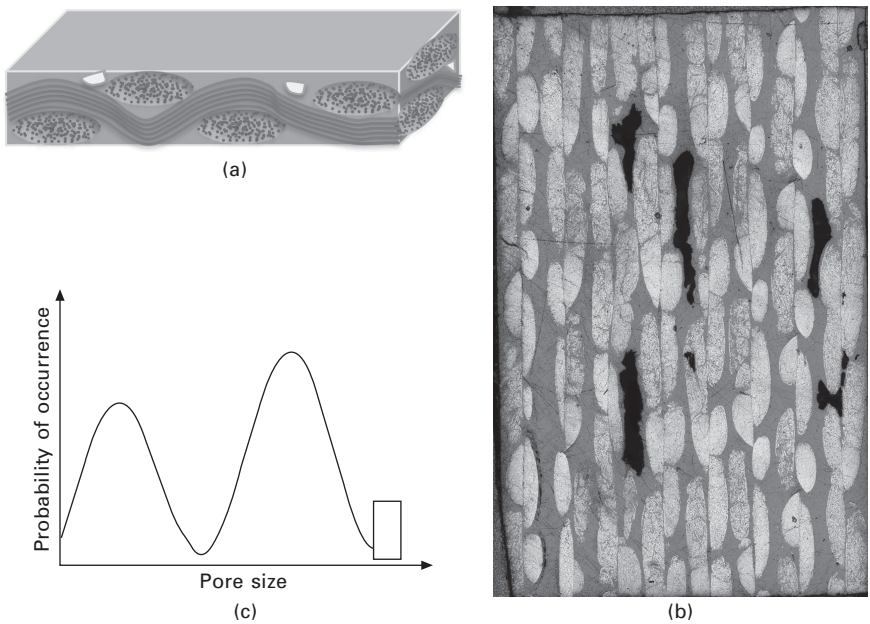

14.1 (a) Representative volume element containing tows, fluid and pores; (b) micrograph of a carbon fibre non-crimp fabric, showing the tows, the matrix, and pores (part thickness is about 6 mm); (c) typical pore size distribution for a reinforcement fabric.

Copyrighted Material downloaded from Woodhead Publishing Online
Delivered by http://www.woodheadpublishingonline.com
EPFL Lausanne (569-11-299)
Sunday, January 29, 2012 6:21:28 AM
IP Address: 128.178.195.215

By similarity with soil mechanics, the fluid phase saturation S is defined as:

$$S = \frac{V_l}{1 - V_f} \qquad 14.2$$

where $(1 - V_f)$ is the initial, dry preform, open porosity; S varies from 0 to 1 between a dry and a fully infiltrated (saturated) preform.

The main descriptors of the dry porous medium are its porosity, its specific surface, and the pore distribution. The fibre volume fraction (complementary of porosity, and most often used in composite practice) is calculated as $V_f = N\Sigma/(\rho_f\ h)$, where N is the number of fabric layers, Σ the areal mass of the fabric, ρ_f the density of the fibre material and h the height of the fabric stack. For a simple arrangement of aligned cylinders, packed on a square array, the maximum fibre volume fraction that can be attained is $V_{fmaxs} = \pi/4$. For a hexagonal array, $V_{fmaxh} = \pi/2\sqrt{3}$.

The specific surface S_f of the porous medium per volume of material is rather difficult to measure as it is also linked to the surface roughness of the reinforcement, and thus its measure depends on the measurement method (Bear, 1972). For composite reinforcements, it can be measured using the BET

© Woodhead Publishing Limited, 2011

(Brunauer, Emmet and Teller) technique based on the physical absorption of gases on a surface (Verrey, 2006), or alternatively it can be estimated using simple geometrical models. For example, it can be assumed that an assembly of parallel rods of radius r lies on a square array, $S_{fs} = 2V_f/r$, or for a hexagonal array, $S_{fh} = 3V_f/r$.

Pore size distribution is a statistical descriptor of the porous medium that is also difficult to measure directly. It is often measured through gradual filling of the media with non-wetting fluids (Bear, 1972, p. 42). As textiles are most often formed of tows or yarns that are assembled into a preform, the porous medium is generally described by a bimodal pore size distribution, as sketched in Fig. 14.1c.

14.2.2 Fundamentals of flow in porous media

The underlying physical phenomena for all composite processes include capillary or surface phenomena, transport of fluid, heat, and mass, the mechanics of preform deformation during infiltration, matrix solidification or chemical cross-linking, and also potential matrix/reinforcement chemical reaction during and after the process. Complete solutions of the flow equations will be described in detail in Chapter 19.

In the following, we consider the general case of infiltration by a liquid of a compressible porous preform in which all initial porosity is interconnected (no closed pores), all attributes typical of textile reinforcements. We do not treat heat or mass transfer (as induced by a chemical reaction) since these are not directly used in defining permeability.

To describe the flow of liquid in a porous medium, averaged values of relevant parameters, such as velocity or volume fraction, are used to derive equations for conservation of mass and momentum, all in a continuum mechanics approach. It is generally assumed that the densities of liquid and solid phases are constant; in most cases of non-compressible liquid fluids, this is a reasonable assumption; on the other hand it should be removed when infiltration by a gas is considered, which complicates the equations somewhat (Scheidegger, 1974).

Mass conservation equations are written for the solid and the fluid phase, respectively, as

$$\frac{\partial V_f}{\partial t} + \nabla (V_f u_s) = 0 \qquad 14.3$$

and

$$\frac{\partial((1 - V_f) S)}{\partial t} + \nabla ((1 - V_f) S u_l) = 0 \qquad 14.4$$

where u_s is the local velocity of the solid, and u_l is the average local velocity of the liquid within the pores.

© Woodhead Publishing Limited, 2011

Copyrighted Material downloaded from Woodhead Publishing Online
Delivered by http://www.woodheadpublishingonline.com
EPFL Lausanne (569-11-299)
Sunday, January 29, 2012 6:21:28 AM
IP Address: 128.178.195.215

The momentum equation is generally written using Darcy's law:

$$(1 - V_f)S(u_l - u_s) = -\frac{K}{\eta}\nabla P \qquad 14.5$$

where K (a function of S and V_f) is the permeability of the porous medium in ΔV, η is the liquid viscosity, and P is the pressure in the liquid. K, the permeability, is thus defined from Eq. 14.5 as a tensorial quantity, with units m^2. Equation 14.5 is written neglecting gravitational or other potential body forces, and is only valid provided the relevant Reynolds number, defined in relation to the average fluid velocity and the pore diameter, is less than about 1: this is most often the case for polymer composite processes because polymers have comparatively high viscosity. The left-hand side of Eq. 14.5 is called the superficial velocity, often also called the filtration velocity, which was initially defined by Darcy as the ratio of the volumetric flow rate Q out of a porous medium, over the cross-section of this porous medium, A (Darcy, 1856). For fully saturated flow in a rigid porous medium, the filtration velocity u_0 is generally simply written as:

$$\frac{Q}{A} = u_0 = (1 - V_f)u_l \qquad 14.6$$

Finally, having neglected inertial and body forces in both solid and liquid, stress equilibrium is written using an extension of the effective stress principle developed for partially saturated soils (Wang, 2000):

$$\nabla\sigma' - \nabla(BS\,P) = 0 \qquad 14.7$$

where σ' is the effective stress acting in the solid, counted as positive in compression and averaged over a surface area comprising both solid and liquid. B is the Biot tensor; if the porous medium is isotropic, then $B = bI$, where I is the identity matrix, and $b = 1 - C_0/C_s$, where C_0 is the compression modulus of the fibre assembly, and C_s is the compression modulus of the fibre material itself. If the porous medium is not isotropic, as is often the case for composite reinforcements, the Biot tensor is still diagonal and all three diagonal terms depend on the compliance tensors of the fibre material, and of the fibre assembly (Tran, 2009). Since the fibre material is generally of very high modulus compared to the compressibility of the fibre bed, $b = 1$ in all directions is often used in composite processing, with very few exceptions (Tran, 2009). Initial and boundary conditions valid for each case complete the definition of the problem.

Four main characteristics of the fibre preform and the fluid thus need to be known for a solution of the problem: the viscosity η, the dependence of the saturation S on the local pressure P, the stress–strain behaviour of the preform, and the permeability K. This last parameter is not only important; it is somewhat special in that it varies strongly with its underlying governing

Copyrighted Material downloaded from Woodhead Publishing Online
Delivered by http://www.woodheadpublishingonline.com
EPFL Lausanne (569-11-299)
Sunday, January 29, 2012 6:21:28 AM
IP Address: 128.178.195.215

© Woodhead Publishing Limited, 2011

parameters: K increases with the square of the average pore diameter, and varies even more strongly with the pore volume fraction; it is thus a crucial parameter in modelling composite fabrication processes.

In the most general case of multiphase flow, permeability as defined in Eq. 14.5 is a function of the preform volume fraction, fibre arrangement and stress state, as well as of the degree of fluid saturation in the preform, S. Following the approach developed in soil science, K is then generally separated into two terms, $K = k_r K_s$. The saturated permeability, K_s, is the permeability tensor of the preform for fully saturated flow, a function of the internal geometry of pores in the reinforcement only. The *relative* permeability, k_r, is a scalar ranging from 0 to 1, which is a function of S. In composite processing, most attention has so far been given to the determination of the saturated permeability, K_s. We will focus on this parameter in the next section, and will then briefly address the issue of relative permeability, k_r.

14.3 Saturated permeability modelling for fibre preforms

14.3.1 Introduction and historical perspective

By definition, the saturated permeability K_s is a characteristic of the preform only, which in principle does not vary with the nature of the infiltrant – provided of course that this infiltrant is an incompressible Newtonian fluid, which furthermore has fully infiltrated all open pores of the preform and flows in the Darcian regime of appropriately low Reynolds number. As indicated earlier, K_s is a tensor, so in principle nine values need to be identified for a three-dimensional case of infiltration:

$$K_s = \begin{pmatrix} K_{11} & K_{12} & K_{13} \\ K_{21} & K_{22} & K_{23} \\ K_{31} & K_{32} & K_{33} \end{pmatrix}$$

For symmetry reasons, $K_{ij} = K_{ji}$, so only six values differ. Finally, if the principal axes of the tensor are found, it is possible to write the permeability tensor with only three distinct elements, K_x, K_y and K_z on the diagonal, all other terms becoming nil (Bear, 1972). For textile fabrics, it is often easy to determine that the axes of the coordinate system should be oriented with x and y in the plane of the fabric, and z corresponding to its thickness. As a result, in the composite community, three values of the saturated permeability tensor are considered, two in plane, and one through the thickness of the reinforcement, following the fabric geometry as shown in Fig. 14.2. It should be noted, however, that the warp and weft directions of the fabric do not necessarily correspond to the principal in-plane axes.

Copyrighted Material downloaded from Woodhead Publishing Online
Delivered by http://www.woodheadpublishingonline.com
EPFL Lausanne (569-11-299)
Sunday, January 29, 2012 6:21:28 AM
IP Address: 128.178.195.215

© Woodhead Publishing Limited, 2011

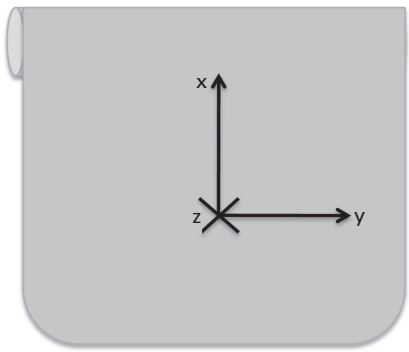

14.2 Schematic of a reinforcement preform and principal axes.

Copyrighted Material downloaded from Woodhead Publishing Online
Delivered by http://www.woodheadpublishingonline.com
EPFL Lausanne (569-11-299)
Sunday, January 29, 2012 6:21:28 AM
IP Address: 128.178.195.215

14.3.2 Continuum mechanics models for dilute and concentrated fibre beds

Capillary tube models

The easiest and earliest model of permeability considers unidirectional fluid flow inside a cylindrical tube of radius R along a direction x parallel to the tube axis. The Hagen–Poiseuille solution of the Navier–Stokes equation in this simple case for the volumetric flow rate is (Bird, 2007):

$$Q = \left(\frac{-\mathrm{d}p/\mathrm{d}x}{2\eta}\right)\left(\frac{\pi R^4}{4}\right), \text{ so } \frac{Q}{A} = -\frac{R^2}{8\eta}\frac{\mathrm{d}p}{\mathrm{d}x} \qquad 14.8$$

Comparing Eq. 14.8 to Eq. 14.5, and considering the tube thickness as negligible, it is clear that $K_s = R^2/8$. This simple relation intuitively shows that permeability is roughly in the order of magnitude of the square of the pore space dimension. In a composite reinforcement, the space between fibres has an order of magnitude of a few microns to a few hundred microns, hence permeability values are expected in the range from 10^{-9} to 10^{-13} m^2. If there are N such tubes per unit area of cross-section normal to the direction of flow, then $V_f = N\pi R^2/1$, and $K_s = (1 - V_f)R^2/8$. These models are of course very limited as the description of the porous medium is far from realistic; in fact this view of flow through porous media is often misleading.

This equation is at the basis of several 'hydraulic radius' models that were developed by 'guessing' an equivalent or average radius describing with sufficient accuracy the porous medium. The most accepted such model is that derived by Kozeny (1927), later modified by Carman (1937, 1956). In the various forms of this model, the porous medium is treated as a bundle of parallel capillary tubes that are not necessarily circular in cross-section. A constant is introduced that depends on the internal geometry of the porous

© Woodhead Publishing Limited, 2011

medium. A well-known form of this equation, very often used in composite literature, is given below:

$$K_s = \frac{r^2}{4k_{i,i}} \frac{(1 - V_f)^3}{V_f^2} \qquad 14.9$$

where r is the fibre radius, V_f the fibre volume fraction, and $k_{i,i}$ the Kozeny–Carman constant ($i = x, y, z$) (Advani, 1994).

The Kozeny–Carman equation is in general reasonably accurate for isotropic porous media (packed particle beds notably) or flow parallel to the axis of parallel fibres, a situation in which it was later re-derived by several authors in the composites literature aiming to arrive at a more precise estimate of k_{ij}. For example, Gebart (1992) derived a similar equation, with $k_{xx} = 1.78125$ for a hexagonal fibre arrangement, and $k_{xx} = 1.65625$ for a square arrangement. On the other hand this estimate does not work well for many other situations, notably for transverse flow through anisotropic fibrous porous media. This is due in particular to the fact that the Kozeny–Carman constant does not take into account the fact that there is a maximum packing volume fraction, at which the permeability drops to 0 for a fibre volume fraction V_f less than unity, at which touching fibres simply block transverse flow. Several authors have proposed to extend the validity of the Kozeny equation (Åström, 1992; Cai, 1993); however, the Kozeny–Carman constant is not known *a priori* and such extensions generally rely on an experimental fit valid only for a given fabric, which furthermore has to depend on flow direction, fibre volume fraction, fibre, fluid and pressure gradient, demonstrating the limits of the model.

Resistance to flow models for a uniform distribution of cylindrical fibres

Another approach to modelling flow in porous media is to consider a fluid, in which spheres or cylinders are suspended without the possibility to move. These suspended solid objects thus present a resistance to flow of the fluid, called a drag force, which can be calculated by solving the Stokes equations for flow of a fluid around a rigid isolated body. Such models are strictly valid only for diluted suspensions, as they do not include the interaction between neighbouring fibres. Happel and Brenner (Bear, 1972) extended this model to treat flow across a less dilute body of cylindrical fibres, introducing a coefficient λ that takes into account the interaction between neighbouring fibres. Several other authors proposed models along these lines, proposing a 'cell' approach, in which the Stokes equations are solved and the geometry of the cell is defined according to a packing geometry, such as quadratic or hexagonal.

For flow *parallel to the fibre axis*, only one fluid velocity component is present, and solutions are found, assuming zero velocity on the fibre surface,

Copyrighted Material downloaded from Woodhead Publishing Online
Delivered by http://www.woodheadpublishingonline.com
EPFL Lausanne (569-11-299)
Sunday, January 29, 2012 6:21:28 AM
IP Address: 128.178.195.215

© Woodhead Publishing Limited, 2011

and zero velocity gradient at the cell surface, situating this mid-way through the liquid, across planes of symmetry. Most models fall along similar lines, with a general equation given as follows by Drummond and Tahir (Jackson, 1986):

$$\frac{K_s}{r^2} = \frac{1}{4V_f}\left(-\ln V_f + K + 2V_f - \frac{V_f^2}{2}\right) \qquad 14.10$$

where K depends on the geometry of the array: $K = -1.476$ for a square array, and $K = -1.354$ for a hexagonal array. This curve is shown together with Eq. 14.9 with the coefficients proposed by Gebart, and the simple initial straight tube model, in Fig. 14.3.

For flow *perpendicular to the fibre axis*, similar solutions have been proposed, which are reviewed by Jackson (1986). Solutions are again very similar, taking the following form:

$$\frac{K_s}{r^2} = \frac{1}{8V_f}(-\ln V_f - 1.476 + 2V_f - 1.774V_f^2 + 4.076V_f^3 + O(V_f^4)) \qquad 14.11$$

for a square array, and:

$$\frac{K_s}{r^2} = \frac{1}{8V_f}(-\ln V_f - 1.490 + 2V_f - 0.5V_f^2 + O(V_f^4)) \qquad 14.12$$

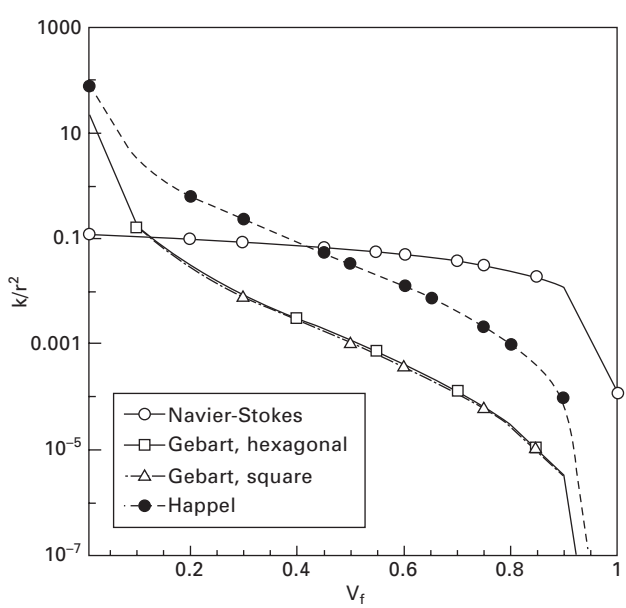

14.3 Reduced permeability as a function of fibre volume fraction, for flow along the fibre axis.

© Woodhead Publishing Limited, 2011

Copyrighted Material downloaded from Woodhead Publishing Online
Delivered by http://www.woodheadpublishingonline.com
EPFL Lausanne (569-11-299)
Sunday, January 29, 2012 6:21:28 AM
IP Address: 128.178.195.215

for a hexagonal array. These curves are shown in Fig. 14.4.

For more concentrated fibre assemblies, nearly all resistance to transverse flow is imposed by the narrowest constriction between two fibres (the well-known 'bottleneck effect'). A solution for flow within this restricted space alone, based on fluid-flow patterns often derived from lubrication theory, coupled with an estimate of the spatial density of such constrictions, leads to a permeability value. Several relevant models based on lubrication theory are found in the literature, which give quite similar results, varying mostly by the assumptions taken to analytically solve the equations. These are found in references by Keller (1964), Sangani (1982), Jackson (1986), Gebart (1992), and Bruschke (1993). The most often used expression in the composite literature is that proposed by Gebart (1992), since it was the first to be presented in a composites journal:

$$\frac{K_s}{r^2} = \frac{16}{9\pi\sqrt{2}}\left(\sqrt{\frac{V_{f\,max\,s}}{V_f}} - 1\right)^{\frac{5}{2}} \qquad 14.13$$

for a quadratic arrangement of cylinders, and

$$\frac{K_s}{r^2} = \frac{16}{9\pi\sqrt{6}}\left(\sqrt{\frac{V_{f\,max\,h}}{V_f}} - 1\right)^{\frac{5}{2}} \qquad 14.14$$

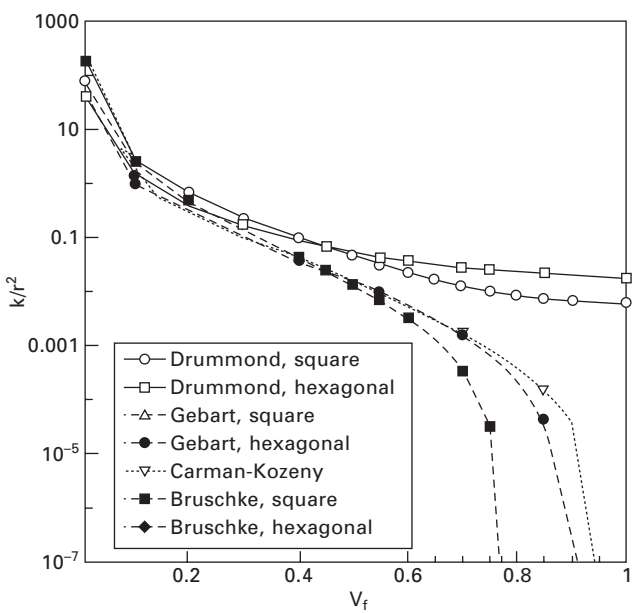

14.4 Reduced permeability as a function of fibre volume fraction, for flow orthogonal to the fibre axis.

© Woodhead Publishing Limited, 2011

Copyrighted Material downloaded from Woodhead Publishing Online
Delivered by http://www.woodheadpublishingonline.com
EPFL Lausanne (569-11-299)
Sunday, January 29, 2012 6:21:28 AM
IP Address: 128.178.195.215

for a hexagonal arrangement of cylinders.

Another development was later proposed by Bruschke (1993) by taking a more accurate geometrical description to solve the flow equations for square arrays:

$$\frac{K_s}{r^2} = \frac{1}{3}\frac{(1-l^2)^2}{l^3}\left(3l\frac{\arctan(\sqrt{(1+l)/(1-l)})}{\sqrt{1-l^2}} + \frac{l^2}{2} + 1\right)^{-1} \qquad 14.15$$

where $l = \sqrt{4V_f/\pi}$, and for hexagonal arrays:

$$\frac{K_s}{r^2} = \frac{1}{3\sqrt{3}}\frac{(1-l_h^2)^2}{l_h^3}\left(3\frac{\arctan(\sqrt{(1+l_h)/(1-l_h)})}{\sqrt{1-l_h^2}} + \frac{l_h^2}{2} + 1\right)^{-1} \qquad 14.16$$

where $l_h = \sqrt{2\sqrt{3}V_f/\pi}$.

Equations 14.13 to 14.16 are also plotted in Fig. 14.4, together with the Carman–Kozeny model with the coefficient chosen so as to obtain the same value as with Eq. 14.14 for $V_f = 0.4$.

Note that in fibre preforms, particularly in woven textiles, there are two 'fibres': the fibres themselves at the finer scale, but also, on a coarser scale at which much of the fluid flow will occur, the woven fibre tows. As a consequence, these models have been extended to elliptical cylinders, which correspond better to the shape of tows used in the composite reinforcements (Labrecque, 1968; Epstein, 1972; Phelan, 1996; Ranganathan, 1996; Papathanasiou, 2002; Markicevic, 2003; Merhi, 2007), or to non-Newtonian fluids (Bruschke, 1993).

More recently, numerical solutions of fluid flow around bundles of cylinders removed the need for several of the above assumptions, and also gave efficient testbed data for evaluation of the validity of the analytical models (Cai, 1993; Berdichevsky, 1993; Gebart 1992; Bruschke, 1993; Nagelhout, 1995; Phelan, 1996). For flow perpendicular to the fibre axes, these showed that Eqs 14.13 to 14.16 are quite accurate in the high volume fraction range of general interest to composite processing. Numerical simulation results are, however, generally limited to simple periodic geometrical units.

14.3.3 Permeability prediction of multi-scale porous media using numerical models

Since most reinforcements are not based on uniformly dispersed fibres, but rather comprise fibre bundles, which are often woven or knitted, there is a need to develop permeability predictions for multi-scale porous media. This has motivated the proposal of several models that rely on a more accurate description of the internal pore geometry in preforms of this type.

Copyrighted Material downloaded from Woodhead Publishing Online
Delivered by http://www.woodheadpublishingonline.com
EPFL Lausanne (569-11-299)
Sunday, January 29, 2012 6:21:28 AM
IP Address: 128.178.195.215

© Woodhead Publishing Limited, 2011

The models vary by the solution method chosen to compute fluid flow through the fabric, but the strategy is often similar. In such models, the representative volume element contains fibre tows that are assumed to either constitute an impermeable solid or have themselves a porous structure. One example of such a unit cell is given in Fig. 14.5. To describe a fabric more accurately, it is also possible to produce a series of different representative unit cells that will then be assembled following a given pattern. Then, the relationship between the flow-rate across the unit cell and the pressure drop is calculated by a numerical method (computational fluid dynamics, or finite element method) or an analytical method (combining analytical solutions of flow inside the tow and in between tows) and a permeability value is thus computed for the cell.

Flow between tows is generally modelled using the Stokes equation:

$$\nabla P = \eta \nabla^2 u_l \qquad 14.17$$

The boundary for flow at the tow surface is often treated as a no-slip boundary for impermeable tows, or by matching fluid velocities and/or pressure at the interface when the tow is permeable. In semi-analytic models, flow within the tow is described using Darcy's law, Eq. 14.5; in some cases, an extension of Darcy's law to high-velocity flow regimes, known as the Brinkman equation, is used instead, often because it presents the advantage of being more easily coupled, in simulations, with the Stokes equation:

$$\langle \nabla P \rangle = -\frac{\eta}{K_s} \langle u_l \rangle + \eta_e \nabla^2 u_l \qquad 14.18$$

The brackets denote (REV) volume average properties, while η_e is an effective viscosity, which is used to match the shear stress values at the interface between the free flowing fluid and the porous medium: $\eta \left.\frac{d\langle u_l \rangle}{dy}\right|_{y=0^+} = \eta_e \left.\frac{d\langle u_l \rangle}{dy}\right|_{y=0^-}$,

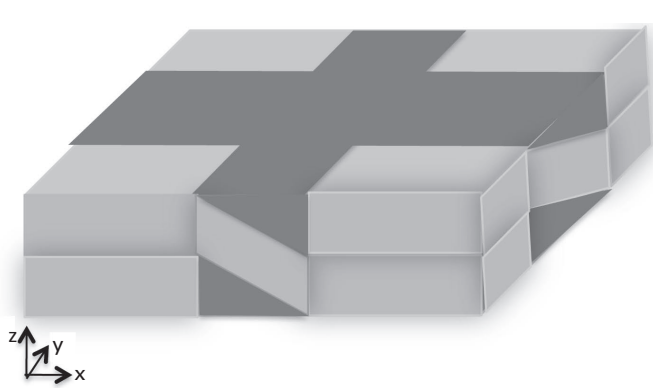

14.5 Schematic of a unit cell used for numerical modelling; channels are dark grey and tows are light grey.

© Woodhead Publishing Limited, 2011

Copyrighted Material downloaded from Woodhead Publishing Online
Delivered by http://www.woodheadpublishingonline.com
EPFL Lausanne (569-11-299)
Sunday, January 29, 2012 6:21:28 AM
IP Address: 128.178.195.215

where $y = 0^+$ represents the boundary on the side of the free-flowing fluid, and $y = 0^-$ represents the boundary on the side of the fibre tow. This was used among others by Ranganathan (1996), Phelan (1996) and Song (2005) to model flow within fibre tows.

Analytical models have also been developed; in this case the unit cell is greatly simplified so that a tractable solution of the equations can be written for flow within the tow and also between tows, the two being then assembled into a full permeability model. Recent examples are by Yu (2000), Lundström (2000b), Endruweit (2011) and Chen (2010). These models are useful for rapid evaluation of the influence of tow permeability, or intra-tow channel size on the permeability. For example, Chen (2010) showed that the in-plane permeability of a woven fabric scales with the third power of the channel width, while the through-thickness permeability scales with the fourth power of this parameter. Such models can also easily demonstrate that several fabrics having similar overall volume fractions of fibre do not have the same permeability.

Many variations of the numerical models are found in the literature (Cai, 1993; Gebart, 1992; Markicevic, 2003; Papathanasiou, 1997, 2002; Verleye, 2008, 2010; Griebel, 2010; Nordlund, 2005, 2006), also extended to the case of non-Newtonian fluid flow (Loix, 2009). These are in general compared to analytical or experimental results, and the agreement is often, beyond the accuracy of the modelling method, related to the accuracy of the fabric description. Alternative models based on lattice Boltzmann methods or smooth particle hydrodynamics (SPH) methods have also been developed, initially at NIST (Spaid, 1997, 1998; Belov, 2004; Comas-Cardona, 2005). These are elegant but remain difficult to use in practice, as the necessary parameters lack a direct relation to physical characteristics of the preforms.

The predictive power of these multi-scale models thus relies on the trade-off between a very accurate description of the porous medium and computation complexity. These models are best if a faithful description of the internal structure of the reinforcement is available. As a result, they are often coupled to unit cell models that describe the internal structure of the textiles, such as those described in Chapters 7 and 8. In addition, it is now possible to account for an evolving fibre distribution in the cell, caused by preform deformation when the fabric is sheared or compressed during the preforming operation. Recently, Verleye *et al.* (2010) compared the speed and accuracy of two methods, one based on a finite-difference solution of Stokes flow in a unit cell, the other using a 2D approximation of the fluid flow path. The Stokes flow solution was found to attain the desired accuracy of 10%, but for several hours of computing, making this solution time consuming. A look-up table with already computed values for a given fabric was proposed to give access to values for K in practical cases.

Finally, the description of the porous medium can also be based on an

Copyrighted Material downloaded from Woodhead Publishing Online
Delivered by http://www.woodheadpublishingonline.com
EPFL Lausanne (569-11-299)
Sunday, January 29, 2012 6:21:28 AM
IP Address: 128.178.195.215

© Woodhead Publishing Limited, 2011

experimental 3D reconstruction of a given textile; as mentioned, this is now feasible using X-ray microtomography, as the current resolution is somewhat below the micrometre using X-ray synchrotron radiation (Desplentere, 2005; Badel, 2008; Koivu, 2010).

14.4 Unsaturated permeability modelling

14.4.1 Relative permeability

This parameter, inherited from soil science treatment of multi-phase flow, represents the additional resistance to fluid flow created when the pore space comprises a third phase, generally air or a gas. It thus depends on the fibre–matrix system, and is much more difficult to measure in the case of composite systems since model fluids cannot be used, or to predict theoretically given the far greater geometrical complexity of non-saturated flow. Therefore, models are mainly semi-empirical. Such models have been proposed and validated experimentally in soil science, and take the general form:

$$k_r = S^n \tag{14.19}$$

where n is an exponent typically between 1 and 3 for particle-based soils (Spitz, 1996) while S is considered here as the saturation in the non-wetting phase (this assumes that the resin is considered in this chapter as the non-wetting phase, but it is possible to consider the inverse case). Alternative models introduce a parameter λ (Brooks, 1964), named the pore size distribution index:

$$k_r = S^2\left(1-(1-S)^{\frac{2+\lambda}{l}}\right) \tag{14.20}$$

or additional parameters L, M and β (Van Genuchten, 1980) that are related to the shape of the S(P) curve :

$$k_r = S^L\left(1-(1-S)^{\frac{1}{M}}\right)^{2M} \tag{14.21}$$

The approach also implies, as indicated in Section 14.2.2, that the saturation curve be measured for the given reinforcement/matrix system (Patel, 1996a, b; Nordlund, 2008). Although this approach is standard in multi-phase flow modelling for other branches of engineering, it has seldom been used toward composite process modelling. There are examples however, that either were based on formulae derived from soil science (Markicevic, 2006; Patel, 1996a,b; Michaud, 1994) or used inverse determination of Eqs 14.19 and 14.21 from experiment (Dopler, 2000; Nordlund, 2008). This is due to the difficulty in evaluating the necessary parameters with the matrix phase, and

Copyrighted Material downloaded from Woodhead Publishing Online
Delivered by http://www.woodheadpublishingonline.com
EPFL Lausanne (569-11-299)
Sunday, January 29, 2012 6:21:28 AM
IP Address: 128.178.195.215

© Woodhead Publishing Limited, 2011

to the fact that most models developed in soil science implicitly assume that capillary forces are independent of fluid velocity, which is not always true when high-viscosity matrices are used (Verrey, 2006).

14.4.2 Alternative methods: use of sink terms

Another approach taken by researchers in the composite field is to consider saturated fluid flow, but introduce pores that will gradually get filled during impregnation, typically representing a tow. In general, flow is assumed to first take place in between the fabric tows, with the resin only penetrating later and more slowly the tows themselves, gradually behind the infiltration front. This implicitly assumes that the fluid does not wet the fabric. In that case, the permeability values are evaluated using saturated models, with one value for the tow permeability, and another value for the overall permeability of the fabric. A sink term is then introduced in the models, providing fairly good agreement when adjusting the saturation rate for tow infiltration (Binetruy, 1997, 1998, 2006; Acheson, 2004; Zhou, 2006; Kuentzer, 2006; Lawrence, 2009; Bréard, 2003; Wolfrath, 2006; Bayldon, 2009). As a result, the overall saturation of the fabric varies with time, but no specific relative permeability model is needed. These models have proven to help solve the issue of permeability evolving during flow progression, but are also heavily reliant on empirical or simplified models, or on the use of experimental values to back-calculate the saturation kinetics.

14.5 Permeability measurement methods

As described in the previous sections, several models have been developed to predict the permeability of an assembly of fibres or tows; however, these are based either on analytical solutions for very simple geometrical descriptions of the pore structure, or on numerical simulations that describe a specific (and often still idealized) pore structure but require one to build a dedicated computer model implying sometimes long computation times. In all cases, validation of the models is crucial; hence it is necessary to confront the models to experimentally measure values of permeability. Also, for practical purposes of composite manufacturing, it is sometimes sufficient to directly measure preform permeability, without the need for a model.

Many experimental methods have been proposed to measure permeability of fibre preforms; since there is no established procedure or norm for permeability testing of reinforcements for composite processing (whereas norms exist for permeability measurement to air of textiles (ISO, 1995), for clothing, industrial textiles, air bags, and of course soils), all researchers have developed in-house methods depending on the fabric type, flow geometry and available funding. As a result, the literature reports many measurement methods and

Copyrighted Material downloaded from Woodhead Publishing Online
Delivered by http://www.woodheadpublishingonline.com
EPFL Lausanne (569-11-299)
Sunday, January 29, 2012 6:21:28 AM
IP Address: 128.178.195.215

© Woodhead Publishing Limited, 2011

results for permeability of fabrics, which are not easily comparable (Sharma, 2010). Parnas *et al*. (1995, 1997) at NIST proposed to use a reference fabric for standardization of permeability measurement methods, and a benchmark exercise was later reported (Lundström, 2000a), where scatter was observed and attributed to differences in specimen preparation. A benchmark exercise is currently running between several laboratories (Laine, 2010; Abter, 2011) with the aim of reaching practical guidelines for permeability measurement as applied to composite reinforcements.

In principle, permeability measurement is rather straightforward: following Darcy's law, Eq. 14.5, if a fluid of known viscosity flows under a known pressure differential through a known thickness and area of porous medium, measurement of the volumetric flow rate leads to the permeability. This is the method proposed by Darcy in 1856. With fibre composites, reinforcements are often highly anisotropic; as a consequence, in measuring the permeability of fibre preforms, flow of the fluid must be directed along selected orientations to arrive at each of the relevant component(s) of the permeability tensor. In practice, this measurement leads to a large variability, because the porous medium itself is statistical in nature (and this is also true for reinforcements used in composites), or because the measurement method leads to many potential variations.

The choice of test fluid is also important: different fluids have been used that ideally have a viscosity close to that of the pre-polymer used in practice. For many cases of liquid composite moulding, thermoset resins are in the viscosity range between 0.3 and 1 Pa.s. As a result, water is never used; rather, several vegetal or mineral oils, corn syrup, dilute polymer solutions (such as PEG solutions), or the resin itself have been used (Sharma, 2010). If the flow is saturated and no capillary effects are present (meaning flow is fully or analogously saturated), all fluids should give the same results, provided each has a stable Newtonian behaviour and does not degrade during flow or react with the reinforcement or its sizing. Temperature control of the fluid during the test is also a crucial point, unfortunately often neglected.

14.5.1 Through-thickness permeability measurement

For through-thickness permeability measurement, techniques used for composite reinforcements are all somewhat similar, being based on unidirectional saturated flow across a stack of reinforcement layers, as shown schematically in Fig. 14.6. This is similar to the methods used in soil science for permeability measurement of granular porous media. The critical point is to prevent edge flow between the porous medium and the container; this is in general addressed by using tight-fitting samples, a side membrane that can be fitted to the preform, or by blocking lateral flow (Merhi, 2007; Wu, 1994; Endruweit, 2002; Ouagne, 2010; Drapier, 2002, 2005; Buntain, 2003;

Copyrighted Material downloaded from Woodhead Publishing Online
Delivered by http://www.woodheadpublishingonline.com
EPFL Lausanne (569-11-299)
Sunday, January 29, 2012 6:21:28 AM
IP Address: 128.178.195.215

© Woodhead Publishing Limited, 2011

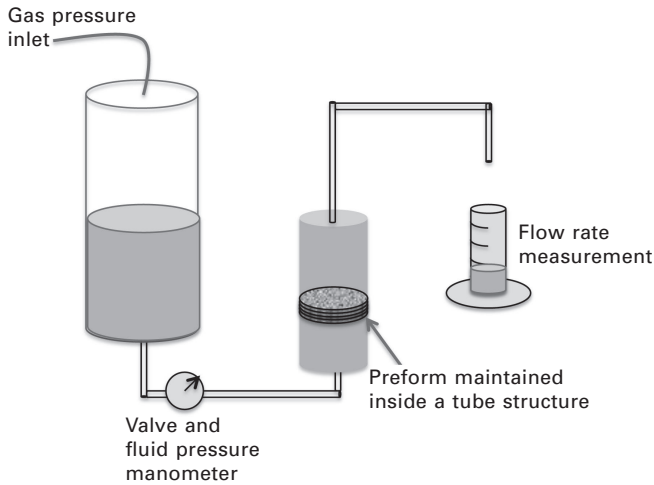

14.6 Schematic of through-thickness permeability measurement.

Comas-Cardona, 2007; Song, 2009). Some authors included the possibility of simultaneously compressing the reinforcement stack in the permeameter device, with a goal of evaluating the change of permeability with volume fraction in a direct measurement (Comas-Cardona, 2007; Buntain, 2003; Ouagne, 2010).

14.5.2 In-plane permeability measurement

In-plane permeability measurement leads to the identification of the two in-plane values of the permeability tensor, K_x and K_y, that are necessary for almost all LCM processes where in-plane flow predominantly takes place. As a result, diverse methods have been proposed, which can be classified into several measurement types (Sharma, 2010; Verleye, 2010): (1) based on the flow geometry, radial versus unidirectional; (2) based on the inlet boundary condition: constant flow rate or constant inlet pressure; and (3) based on the type of flow: saturated continuous flow, or transient filling of the reinforcement, generally called 'unsaturated' measurement. In saturated unidirectional measurements, the permeability is calculated directly from Eq. 14.5 as:

$$K_s = \frac{-Q\eta L_{tot}}{A\,\Delta P} \qquad 14.22$$

where L_{tot} is the length of the preform in the direction of flow, A its cross-section, and ΔP the pressure difference in the fluid between outlet and inlet (hence negative), generally measured by a pressure transducer at the flow inlet.

Copyrighted Material downloaded from Woodhead Publishing Online
Delivered by http://www.woodheadpublishingonline.com
EPFL Lausanne (569-11-299)
Sunday, January 29, 2012 6:21:28 AM
IP Address: 128.178.195.215

© Woodhead Publishing Limited, 2011

In unsaturated unidirectional measurements, monitoring of the flow front position with time, $L(t)$ is used to compute permeability, based on integration of Eq. 14.5 with the mass conservation equation (Eq. 14.4), assuming saturated flow. The flow front position is most often measured by visual monitoring through a transparent mould as shown in Fig. 14.7 (Ferland, 1996; Verrey, 2006). Alternative methods have also been proposed, using fibre optic sensors (Ahn, 1995), thermistors (Weitzenböck, 1998), pressure transducers (Endruweit, 2006), or electrical resistance measurements (Luthy, 2001). If flow is under constant applied pressure at the inlet, it is shown that $L^2(t)/t = \psi^2$ is a constant, which is experimentally measured as the slope of the $L^2(t)$ versus t curve, and the overall permeability K is measured as:

$$K = \frac{-(1 - V_f)\eta\psi^2}{2\Delta P} \qquad 14.23$$

where ΔP is the (constant) pressure difference in the fluid between the flow front and the inlet (Michaud, 2001).

If flow is forced to proceed at a constant flow rate, then $L(t) = \frac{Q}{A(1 - V_f)}t$ (the flow front position varies linearly with time), and the inlet pressure increases with time, so that:

$$K = \frac{-Q^2\eta}{A^2(1 - V_f)\Delta P}t \qquad 14.24$$

where ΔP is the pressure difference between inlet and outlet at instant t. To evaluate ΔP, an assumption that is often made is to neglect the capillary pressure at the flow front, and set the front pressure to the gas pressure in

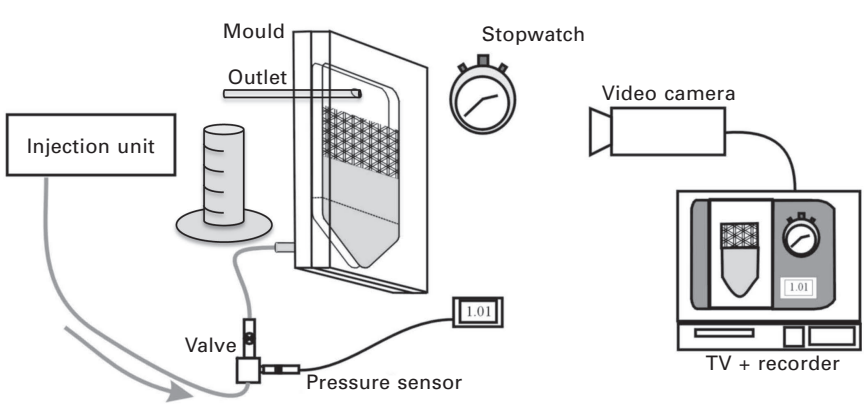

14.7 Schematic of in-plane permeability measurements, allowing both measurement methods, through flow front monitoring, for unsaturated measurements, and through flow rate measurement after complete filling, for saturated measurements.

Copyrighted Material downloaded from Woodhead Publishing Online
Delivered by http://www.woodheadpublishingonline.com
EPFL Lausanne (569-11-299)
Sunday, January 29, 2012 6:21:28 AM
IP Address: 128.178.195.215

© Woodhead Publishing Limited, 2011

the preform ahead of the infiltration front. This has led to the observation that the overall permeability K measured this way is often different from K_s measured in a saturated flow experiment and depends on the model fluid used (De Parseval, 1997; Pillai, 1998, 2004; Slade, 2001; Tan, 2007; Bréard, 2003; Verleye, 2010). The discrepancy appears greater for fabrics with wider pore size distributions, for example woven fabrics versus random fibre mats (Pillai, 2004). This is related to the wetting characteristics of the fluid as compared to air: according to Eq. 14.19, the permeability value K is reduced by a factor $k_r < 1$ when the fluid is not wetting, and increased when the fluid is wetting (as we considered saturation in non-wetting fluid in Eq. 14.19). Moreover, an overall measurement of K thus depends on the potentially changing saturation level during the experiment. As a result, it is advised to prefer saturated flow experiments if one seeks to measure the 'true' saturated permeability. Unsaturated flow measurements are nonetheless often used for practical assessment of the flow kinetics, which is fairly accurate provided the test fluid is close in properties (viscosity, surface tension) to the resin used in the composite process.

If the principal directions of the fabric are not known *a priori*, three measurements are needed in three different in-plane directions to obtain the two in-plane principal permeabilities and their orientation axes. To gain time, with fabric preforms, the *in-plane* permeability is often measured by infiltrating the model fluid through a central hole in a thin fibre preform made of the fibre lay-up of interest clamped within a flat transparent mould. The progression of the resulting elliptical flow front, directly showing the principal directions of the fabric, is measured using a CCD camera, and the two principal values of the permeability tensor in this plane are deduced from Darcy's law and the mass conservation equations solved in cylindrical coordinates (Adams, 1987, 1988; Wang, 1994; Weitzenböck, 1999a, b; Lekakou, 1996; Parnas, 2000; Liu, 2007). This relatively easy experiment may, however, again lead to erroneous measurement because of the potential influence of capillarity. Alternative methods for permeability measurement with planar flow use an array of pressure sensors, distributed at several locations close to the surface of the mould, to monitor the fluid pressure at these locations during the test, instead of the flow front. This *a priori* alleviates the capillary issues (Liu, 2007; Wietgrefe, 2010). Advantages of the radial flow experiments are the lack of race-tracking flow at the edges between the fabric and the mould, and the rapid identification of the principal directions of the permeability tensor.

Comparison of results for in-plane permeability measurements shows that the measurement method is not consistent yet, and leads to very scattered results (Laine, 2010; Gommer, 2009; Abter, 2011). Several reasons have been identified, in addition to potential issues of test fluid viscosity change during the experiments. A major reason is the intrinsic variability of the

Copyrighted Material downloaded from Woodhead Publishing Online
Delivered by http://www.woodheadpublishingonline.com
EPFL Lausanne (569-11-299)
Sunday, January 29, 2012 6:21:28 AM
IP Address: 128.178.195.215

© Woodhead Publishing Limited, 2011

fabrics, which has been demonstrated in several studies to be a dominant factor (Hoes, 2004; Lundström, 2000a). As a result, permeability values should be considered as a statistical measurement, and a large number of experiments are required to precisely measure the statistical parameters. Another major reason is a high probability of experimental errors, due for example to manual fabric cutting and placement, to mould deflection during flow, to uncontrolled fabric compression during flow if pressure is high, to race tracking, or to errors in the flow position or fluid pressure measurements. Permeability measurement thus still remains a difficult task, with errors within a factor of 2 often encountered. A potentially valuable method to calibrate measurements is to use a stiff reference porous medium of well-known permeability (Morren, 2009; Vechart, 2010).

14.5.3 Gas permeability measurement

The methods described above apply when the test fluid is a viscous liquid. If the porous medium is sensitive to fluids, for example as may be the case with natural cellulose-based fibre mats (Pettersson, 2006) or biological tissues, or if the fabric already contains a fluid phase as for prepregs (Sequeira-Tavares, 2009), it may become necessary to use gas as the test fluid. Equations for flow and mass conservation of the gas phase are similar, but the gas phase is compressible. Solutions have been developed again in soil science (Van Groenewoud, 1968; Stonestrom, 1989; Shan, 1992). The permeability is quite readily measured by placing the porous medium between two gas chambers, one kept at a given pressure P_a, the other one left to equilibrate from an initial pressure P_i, different from P_a, until P_a is reached. The permeability k is then obtained as (Li, 2004; Sequeira-Tavares, 2009):

$$\ln\left[\frac{(P_a + P(t))(P_a - P_i)}{(P_a - P(t))(P_a + P_i)}\right] = \frac{kAP_a}{\mu_a ZV}t \qquad 14.25$$

where A is the-cross section of the porous medium, Z its thickness, V the volume of the gas chamber of initial pressure P_i, and μ_a the viscosity of the gas phase. The measured value of permeability is the slip-enhanced permeability, as there may be slip effects at the reinforcement surface, also known as Klinkenberg or Knudsen effects, which alter the value. By conducting several experiments at various levels of pressure, the saturated permeability value can be obtained as $k = K_s\left(1 - \frac{b}{P}\right)$, where b is a parameter of the porous medium, deduced from experiments (Wu, 1998; Tanikawa, 2009; Bear, 1972).

Copyrighted Material downloaded from Woodhead Publishing Online
Delivered by http://www.woodheadpublishingonline.com
EPFL Lausanne (569-11-299)
Sunday, January 29, 2012 6:21:28 AM
IP Address: 128.178.195.215

© Woodhead Publishing Limited, 2011

14.6 Conclusion and future trends

This chapter was intended to provide insight into the theoretical and experimental methods previously and currently used for assessing the permeability of textile reinforcements. Permeability is a key parameter in liquid composite moulding processes; it is a well-defined concept, but still a difficult parameter to quantify, in large part because textile reinforcements are not constant in their internal geometry. As a result, statistical variations should be taken into account, both in the models and in the experimental methods. In addition, the fibre distribution inside a unit cell of fabric is not uniform, and depends on the stress-state of the fabric, so that permeability should also be defined as a function of the stress-state of the textile preform (compression, shear, etc.). Surface tension effects also play a role when unsaturated flow is used to measure permeability, and an adequate method to extract the saturated value from unsaturated experiments is still lacking. Progress is nonetheless observed, on the modelling side thanks to the improvement of computational fluid dynamics methods using real descriptions of the fabric unit cell, and on the experimental side as best practice methods are progressively introduced to standardize the set-ups and analysis. As a result, a large palette of possible modelling methods is now available, depending on the level of precision one seeks to attain: simple analytical models provide quick first estimates, more advanced numerical models based on a precise unit cell description provide accurate data, and complete statistical models, based on a statistical description of the fabric unit cell coupled with simulations, should provide the most realistic picture. Finally, these models should eventually be always coupled to those simulating the unit cell geometrical change with the local stress-state and/or temperature in the mould, so as to map more precisely the local permeability variations during processing of a part.

Copyrighted Material downloaded from Woodhead Publishing Online
Delivered by http://www.woodheadpublishingonline.com
EPFL Lausanne (569-11-299)
Sunday, January 29, 2012 6:21:28 AM
IP Address: 128.178.195.215

14.7 References and further reading

(Abter, 2011) Abter, R. *et al.*, Experimental determination of the permeability of textiles, a benchmark exercise. *Composites Part A*, 42: 1157.

(Acheson, 2004) Acheson, J.A., P. Simacek, and S.G. Advani, The implications of fiber compaction and saturation on fully coupled VARTM simulation. *Composites Part A*, 35: 159.

(Adams, 1987) Adams, K.L., and L. Rebenfeld, In-plane flow of fluids in fabrics: structure/flow characterization. *Text Res J* 57(11): 647–654.

(Adams, 1988) Adams, K.L., W.B. Russel, and L. Rebenfeld, Radial penetration of a viscous liquid into a planar anisotropic porous medium. *Int J Multiphase Flow* 14(2): 203–215.

(Advani, 1994) Advani, S.G., ln *Flow and Rheology in Polymer Composites Manufacturing*, ed. R.B. Pipes, Elsevier, Vol. 10, p. 591.

(Ahn, 1995) Ahn, S.H., W.I. Lee, and G.S. Springer, Measurement of the three-dimensional

© Woodhead Publishing Limited, 2011

permeability of fiber preforms using embedded fiber optic sensors. *J Comp Mater* 29(6): 714–733.

(Åström, 1992) Åström, B.T., R.B. Pipes, and S.G. Advani, On flow through aligned fiber beds and its application to composites processing. *J Comp Mater* 26(9): 1351–1373.

(Badel, 2008) Badel, P., E. Vidal-Sallé, E. Maire, and P. Boisse, Simulation and tomography analysis of textile composite reinforcement deformation at the mesoscopic scale. *Comp Sci Technol* 68: 2433–2440.

(Bayldon, 2009) Bayldon, J.M., and I.M. Daniel, Flow modeling of the VARTM process including progressive saturation effects. *Composites Part A* 40: 1044.

(Bear, 1972) Bear, J., *Dynamics of Fluids in Porous Media*, Dover Publications, New York.

(Belov, 2004) Belov, E.B., S.V. Lomov, I. Verpoest, T. Peters, D. Roose, R.S. Parnas, K. Hoes and H. Sol, Modelling of permeability of textile reinforcements: lattice Boltzmann method. *Comp Sci Technol* 64: 1069.

(Berdichevsky, 1993) Berdichevsky, A.L., and Z. Cai, Preform permeability predictions by self-consistent method and finite element simulation. *Polym Comp*, 14(2): 132–143.

(Binetruy, 1997) Binetruy, C., B. Hilaire, and J. Pabiot, The interactions between flows ocurring inside and outside fabric tows during RTM. *Comp Sci and Technol* 57: 587–596.

(Binetruy, 1998) Binetruy, C., B. Hilaire, and J. Pabiot, Tow impregnation model and void formation mechanisms during RTM. *J Comp Mater*, 32(3): 223–245.

(Binetruy, 2006) Binetruy, C., B. Gourichon, and P. Krawczak, Experimental investigation of high fiber tow count fabric unsaturation during RTM. *Comp Sci Technol* 66: 976.

(Bird, 2007) Bird, R.B., W.E. Stewart, and E.N. Lightfoot, *Transport Phenomena*, revised 2nd edition, Wiley, Chichester, UK.

(Bréard, 2003) Bréard, J., Y. Henzel, F. Trochu, and R. Gauvin, Analysis of dynamic flows through porous media. Part I: Comparison between saturated and unsaturated flows in fibrous reinforcements. *Polym Comp*, 24: 391.

(Brooks, 1964) Brooks, R.H., and A.T. Corey, Hydraulic properties of porous media. *Colorado State University Hydrology Papers*, p. 27.

(Bruschke, 1993) Bruschke, M.V., and S.G. Advani, Flow of generalized Newtonian fluids across a periodic array of cylinders. *J Rheology*, 37(3): 479–498.

(Buntain, 2003) Buntain, M.J., and S. Bickerton, Compression flow permeability measurement: a continuous technique. *Composites Part A* 34: 445.

(Cai, 1993) Cai, Z., and A.L. Berdichevsky, An improved self-consistent method for estimating the permeability of a fiber assembly. *Polym Comp*, 14(4): 314–323.

(Carman, 1937) Carman, P.C., Fluid flow through granular beds. *Trans Inst Chem Eng* 15: 150.

(Carman, 1956) Carman, P.C., *Flow of Gases through Porous Media*, Butterworths Scientific Publications, London.

(Chen, 2010) Chen, Z.R., L. Ye, and M. Lu, Permeability predictions for woven fabric preforms. *J Comp Mater*, 44(13): 1569–1586.

(Comas-Cardona, 2005) Comas-Cardona, S., P. Groenenboom, C. Binetruy, A generic mixed FE-SPH method to address hydro-mechanical coupling in liquid composite moulding processes. *Composites Part A* 36(7): 1004–1010.

(Comas-Cardona, 2007) Comas-Cardona, S., C. Binetruy, and P. Krawczak, Unidirectional compression of fibre reinforcements. Part 2: A continuous permeability tensor measurement. *Comp Sci Technol* 67: 638.

Copyrighted Material downloaded from Woodhead Publishing Online
Delivered by http://www.woodheadpublishingonline.com
EPFL Lausanne (569-11-299)
Sunday, January 29, 2012 6:21:28 AM
IP Address: 128.178.195.215

© Woodhead Publishing Limited, 2011

(Darcy, 1856) Darcy, H., *Les Fontaines Publiques de la Ville de Dijon*. Victor Dalmont, Paris.

(De Parseval, 1997) De Parseval, Y., K.M. Pillai, and S.G. Advani, Simple model for the variation of permeability due to partial saturation in dual scale porous media. *Transport in Porous Media* 27: 243.

(Desplentere, 2005) Desplentere, F., S.V. Lomov, D.L. Woerdeman, I. Verpoest, M. Wevers, and A. Bogdanovich, Micro-CT characterization of variability in 3D textile architecture. *Comp Sci Technol* 65: 1920–1930.

(Dopler, 2000) Dopler, T., A. Modaressi, and V.J. Michaud, Simulation of metal composite isothermal infiltration processing. *Metall Mater Trans* 31B: 225–233.

(Drapier, 2002) Drapier, S., A. Pagot, A. Vautrin, and P. Henrat, Influence of the stitching density on the transverse permeability of non-crimped new concept (NC2) multiaxial reinforcements: measurements and predictions. *Comp Sci Technol*, 62: 1979.

(Drapier, 2005) Drapier, S., J. Monatte, O. Elbouazzaoui, and P. Henrat, Characterization of transient through-thickness permeabilities of Non Crimp New Concept (NC2) multiaxial fabrics. *Composites Part A* 36: 877.

(Dullien, 1979) Dullien, F.A.L., *Porous Media, Fluid Transport and Pore Structure*, Academic Press, New York.

(Endruweit, 2002) Endruweit, A., T. Luthy, and P. Ermanni, Investigation of the influence of textile compression on the out-of-plane permeability of a bidirectional glass fiber fabric. *Polym Comp* 23(4): 538–554.

(Endruweit, 2006) Endruweit, A., P. McGregor, A.C. Long, and M.S. Johnson, Influence of the fabric architecture on the variations in experimentally determined in-plane permeability values. *Comp Sci Technol* 66(11–12): 1778–1792.

(Endruweit, 2011) Endruweit, A., and A.C. Long, A model for the in-plane permeability of triaxially braided reinforcements. *Composites Part A* 42: 165–172.

(Epstein, 1972) Epstein, N., and J. Masliyah, Creeping flow through clusters of spheroids and elliptical cylinders. *Chem Eng J* 3: 169–175.

(Ferland, 1996) Ferland, P., D. Guittard, and F. Trochu, Concurrent methods for permeability measurement in resin transfer molding. *Polym Comp*, 17(1): 149–158.

(Gebart, 1992) Gebart, B.R., Permeability of unidirectional reinforcement for RTM. *J Comp Mater*, 26(8): 1100–1133.

(Gommer, 2009) Gommer, F., S. Lomov, K. Vandenbosche, *et al.*, Error assessment in permeability measurement using radial flow method. *Adv Comp Lett*, 18(4): 123–130.

(Griebel, 2010) Griebel, M., and M. Klitz, Homogenization and numerical simulation of flow in geometries with textile microstructures. *Multiscale Modelling and Simulation* 8(4): 1439–1460.

(Gutowski, 1987) Gutowski, T.G., *et al.*, Consolidation experiments for laminate composites. *J Comp Mater* 21: 650–669.

(Hoes, 2004) Hoes, K., D. Dinescu, H. Sol, *et al.*, Study of nesting induced scatter of permeability values in layered reinforcement fabrics. *Composites Part A* 35(12): 1407–1418.

(ISO, 1995) ISO 9237, Textiles, determination of the permeability of fabrics to air.

(Jackson, 1986) Jackson, G.W., and D.F. James, The permeability of fibrous porous media. *Can J Chem Eng*, 64: 364–374.

(Keller, 1964) Keller, J.B., Viscous flow through a grating or lattice of cylinders. *J Fluid Mech*, 18: 94–96.

(Koivu, 2010) Koivu, V., M. Decain, C. Geindreau, *et al.*, Transport properties of

Copyrighted Material downloaded from Woodhead Publishing Online
Delivered by http://www.woodheadpublishingonline.com
EPFL Lausanne (569-11-299)
Sunday, January 29, 2012 6:21:28 AM
IP Address: 128.178.195.215

© Woodhead Publishing Limited, 2011

heterogeneous materials. Combining computerised X-ray micro-tomography and direct numerical simulations. *Int J Comp Fluid Dyn* 23(10): 713–721.

(Kozeny, 1927) Kozeny, J., Über Kapillare Leitung des Wassers in Boden. *Sitzungsberichte Akad Wiss Wien Math Naturwiss* Kl., Abt 2a, 136: 271–306 (in German).

(Kuentzer, 2006) Kuentzer, N., P. Simacek, S.G. Advani, and S.Walsh, Permeability characterization of dual scale fibrous porous media. *Composites Part A* 37: 2057–2068.

(Labrecque, 1968) Labrecque, R., The effects of fiber cross-sectional shape on the resistance to the flow of fluids through fiber mats. *TAPPI* 51: 8–15.

(Laine, 2010) Laine, B. *et al.*, Experimental determination of textile permeability, a benchmark exercise. Paper 87, *10th Int Conf on Flow Processes in Composite Materials (FPCM10)*, Switzerland, 11–15 July 2010.

(Lawrence, 2009) Lawrence, J.M., V. Neacsu, and S.G. Advani, Modeling the impact of capillary pressure and air entrapment on fiber tow saturation during resin infusion in LCM. *Composites Part A* 40: 1053–1064.

(Lekakou, 1996) Lekakou, C., *et al.*, Measurement techniques and effects on in-plane permeability of woven cloths in resin transfer molding. *Composites Part A* 27: 401–408.

(Li, 2004) Li, H.L., J.J. Jiao, and M. Luk, A falling-pressure method for measuring air permeability of asphalt in laboratory. *J Hydrol* 286(1–4): 69–77.

(Liu, 2007) Liu, Q., R. Parnas, and H. Giffard, New set-up for in-plane permeability measurement. *Composites Part A* 38: 954–962.

(Loix, 2009) Loix, F., L. Orgeas, C. Geindreau, *et al.*, Flow of non-Newtonian liquid polymers through deformed composites reinforcements. *Comp Sci Technol*, 69(5): 612–619.

(Lundström, 2000a) Lundström, T.S., R. Stenberg, R. Bergström, H. Partanen, and P.A. Birkeland, In-plane permeability measurements: a Nordic round-robin study. *Composites Part A* 31(1): 29–43.

(Lundström, 2000b) Lundström, T.S., The permeability of non-crimped stitched fabrics. *Composites Part A* 31: 1345–1353.

(Luthy, 2001) Luthy, T., M. Landert, and P. Ermanni, 1D-permeability measurements based on ultrasound and linear direct current resistance monitoring techniques. *J Mater Process Manu* 10(1): 25–43.

(Markicevic, 2003) Markicevic, B, and T.D. Papathanasiou, An explicit physics-based model for the transverse permeability of multi-material dual porosity fibrous media. *Transport in Porous Media* 53(3): 265–280.

(Markicevic, 2006) Markicevic, B., and N. Djilali, Two-scale modeling in porous media: relative permeability prediction. *Phys Fluids* 18: 033101.

(Merhi, 2007) Merhi, D., V. Michaud, L. Kampfer, P. Vuilliomenet, and J.-A.E. Månson, Transverse permeability of chopped fiber bundle beds: effect of an elliptical bundle cross-section. *Composites Part A* 38: 739–746.

(Michaud, 1994) Michaud, V.J., L. Compton, and A. Mortensen, Capillarity in isothermal infiltration of alumina fiber preforms with aluminum. *Metall Trans* 25A(10): 2145–2152.

(Michaud, 2001) Michaud, V., and A. Mortensen, Infiltration processing of fiber reinforced composites: governing phenomena. *Composites Part A*, 32: 981–996.

(Morren, 2009) Morren, G., M. Bottiglieri, S. Bossuyt, *et al.*, A reference specimen for permeability measurements of fibrous reinforcements for RTM. *Composites Part A* 40(3): 244–250.

Copyrighted Material downloaded from Woodhead Publishing Online
Delivered by http://www.woodheadpublishingonline.com
EPFL Lausanne (569-11-299)
Sunday, January 29, 2012 6:21:28 AM
IP Address: 128.178.195.215

© Woodhead Publishing Limited, 2011

(Mortensen, 1994) Mortensen, A., and I. Jin, Solidification processing of metal matrix composites. *Int Mater Rev* 37(3): 101–128.

(Mortensen, 2000) Mortensen, A., Melt infiltration of metal matrix composites. In: Kelly, A. and Zweben, C., eds, *Comprehensive Composite Materials, Volume 3*, Pergamon Press, Oxford, UK, pp. 521–554.

(Nagelhout, 1995) Nagelhout, D., M.S. Bhat, J.C. Heinrich, *et al.*, Permeability for flow normal to a sparse array of fibers. *Mater Sci Eng A* 191(1–2): 203–208.

(Nordlund, 2005) Nordlund, M., and T.S. Lundström, Numerical study of the local permeability of non-crimp fabrics. *J Comp Mater*, 39: 10.

(Nordlund, 2006) Nordlund M., T.S. Lundström, V. Frishfelds, and A. Jakovics, Permeability network model for non-crimp fabrics. *Composites Part A* 37: 828–835.

(Nordlund, 2008) Nordlund, M., V. Michaud, and J.-A.E. Månson, Experimental method to determine drainage curves in dual-scale fiber reinforcements. *Proc FPCM 9*, Montreal, July 2008.

(Ouagne, 2010) Ouagne, P., and J. Bréard, Continuous transverse permeability of fibrous media. *Composites Part A* 41: 1.

(Papathanasiou, 1997) Papathanasiou, T.D., On the effective permeability of square arrays of permeable fiber tows. *Int J Multiphase Flow* 23(1): 81–92.

(Papathanasiou, 2002) Papathanasiou, T.D., *et al.*, Non-isotropic structured fibrous media: The permeability of arrays of fiber bundles of elliptical cross section. *Polym Comp*, 23(4): 520–529.

(Parnas, 1995) Parnas, R., *et al.*, Permeability characterization. Part 1: A proposed standard reference fabric for permeability. *Polym Comp* 16(6): 429–445.

(Parnas, 1997) Parnas, R., K.M. Flynn, and M.E. Dal-Favero, A permeability database for composites manufacturing. *Polym Comp* 18(5): 623–633.

(Parnas, 2000) Parnas, R., *Liquid Composite Molding*, Hanser Verlag, Munich.

(Patel, 1996a) Patel, N., and L.J. Lee., Modeling of void formation and removal in liquid composite molding. Part I: Wettability analysis. *Polym Comp* 17(1): 96–103.

(Patel, 1996b) Patel, N., and L.J. Lee, Modeling of void formation and removal in liquid composite molding. Part II: Model development and implementation. *Polym Comp* 17(1): 104–114.

(Pettersson, 2006) Pettersson, P., T.S. Lundström, and T. Wikström, A method to measure the permeability of dry fiber mats. *Wood and Fiber Science*, 38(3): 417–426.

(Phelan, 1996) Phelan, F.R., and G. Wise, Analysis of transverse flow in aligned fibrous porous media. *Composites Part A* 27(1): 25–34.

(Pillai, 1998) Pillai, K.M., and S.G. Advani, Model for unsaturated flow in woven fiber preforms during mold filling in resin transfer molding. *J Comp Mater* 32: 1753.

(Pillai, 2004) Pillai, K., Modeling the unsaturated flow in liquid composite molding processes: a review and some thoughts. *J Comp Mater*, 38: 2097–2118.

(Ranganathan, 1996) Ranganathan, S., F.R. Phelan, and S.G. Advani, A generalized model for the transverse fluid permeability in unidirectional fibrous media. *Polym Comp*, 17(2): 222–230.

(Sangani, 1982) Sangani, A.S., and A. Acrivos, Slow flow past periodic arrays of cylinders with application to heat transfer. *Int J Multiphase Flow* 8(3): 193–206.

(Scheidegger, 1974) Scheidegger, A.E., *The Physics of Flow through Porous Media*, 3rd edn. University of Toronto Press, Toronto, Ontario.

(Sequeira-Tavares, 2009) Sequeira-Tavares, S., V. Michaud, and J.A.-E. Månson, Through thickness air permeability of prepregs during cure. *Composites Part A* 40(10): 1587–1596.

Copyrighted Material downloaded from Woodhead Publishing Online
Delivered by http://www.woodheadpublishingonline.com
EPFL Lausanne (569-11-299)
Sunday, January 29, 2012 6:21:28 AM
IP Address: 128.178.195.215

© Woodhead Publishing Limited, 2011

(Shan, 1992) Shan, C., R.W. Falta, and I. Javandel, Analytical solutions for steady-state gas-flow to a soil vapor extraction well. *Water Resour Res* 28(4): 1105–1120.

(Sharma, 2010) S. Sharma, D. A. Siginer, Permeability measurement methods in porous media of fiber reinforced composites. *Appl Mech Rev* 63: 020802.

(Slade, 2001) Slade, J., K.M. Pillai, and S.G. Advani, Investigation of unsaturated flow in woven, braided and stitched fiber mats during mold-filling in resin transfer molding. *Polym Comp* 22: 491.

(Song, 2005) Song, Y.S., K. Chung, T.J. Kang, and J.R. Youn, Numerical prediction of permeability tensor for three dimensional circular braided preform, by considering intra-tow flow. *Polymers and Polymer Composites*, 13: 323–334.

(Song, 2009) Song, Y.S., D. Heider, and J.R. Youn, Statistical characteristics of out-of-plane permeability for plain-woven structure. *Polym Comp* 30(10): 1465–1472

(Spaid, 1997) Spaid, M.A.A., and F.R. Phelan, Lattice Boltzmann methods for modeling microscale flow in fibrous porous media. *Phys Fluids* 9(9): 2468–2474.

(Spaid, 1998) Spaid, M.A.A., and F.R. Phelan, Modeling void formation dynamics in fibrous porous media with the lattice Boltzmann method. *Composites Part A* 29(7): 749–755.

(Spitz, 1996) Spitz, K., and J. Moreno, *A Practical Guide to Groundwater and Solute Transport Modeling*. John Wiley & Sons, New York.

(Stonestrom, 1989) Stonestrom, D.A., and J. Rubin, Air permeability and trapped-air content in two soils. *Water Resour Res* 25(9): 1959–1969.

(Tan, 2007) Tan, H., T. Roy, and K.M. Pillai, Variations in unsaturated flow with flow direction in resin transfer molding: an experimental investigation. *Composites Part A* 38: 1872.

(Tanikawa, 2009) Tanikawa, W., and T. Shimamoto, Comparison of Klinkenberg-corrected gas permeability and water permeability in sedimentary rocks. *Int J Rock Mech Min* 46(2): 229–238.

(Tran, 2009) Tran, T., C. Binetruy, S. Comas-Cardona, and N.-E. Abriak, Microporomechanical behavior of perfectly straight unidirectional fiber assembly: Theoretical and experimental. *Comp Sci Technol*, 69(2): 199–206.

(Van Genuchten, 1980) Van Genuchten, M.T., A closed form for predicting the hydraulic conductivity of unsaturated soils. *Soil Sci Soc Am J* 44: 892–898.

(Van Groenewoud, 1968) Van Groenewoud, H., Methods and apparatus for measuring air permeability of soil. *Soil Sci* 106(4): 275–279.

(Vechart, 2010) Vechart, A.P., R. Masoodi, and K.M. Pillai, Design and evaluation of an idealized porous medium for calibration of permeability measuring device. *Adv Comp Lett*, 19(1): 35–49.

(Verleye, 2008) Verleye, B., R. Croce, M. Griebel, M. Klitz, S. Lomov, G. Morren, H. Sol, I. Verpoest, and D. Roose, Permeability of textile reinforcements: Simulation, influence of shear and validation. *Comp Sci Technol* 68: 2804–2810.

(Verleye, 2010) Verleye, B., S. Lomov, A. Long, I. Verpoest, and D. Roose, Permeability prediction for the meso–macro coupling in the simulation of the impregnation stage of resin transfer moulding. *Composites Part A* 41: 29–35.

(Verrey, 2006) Verrey, V., V. Michaud and J.-A.E. Månson, Dynamic capillary effects in liquid composite molding with non-crimped fabrics. *Composites Part A* 37(1): 92–102.

(Wang, 1994) Wang, T.J., C.-H. Wu, and L.J. Lee, In-plane permeability measurement and analysis in liquid composite molding. *Polym Comp*; 15(4): 278–288.

(Wang, 2000) Wang, H.F., *Theory of Linear Poroelasticity with Applications to Geomechanics and Hydrogeology*. Princeton University Press, Princeton, NJ.

Copyrighted Material downloaded from Woodhead Publishing Online
Delivered by http://www.woodheadpublishingonline.com
EPFL Lausanne (569-11-299)
Sunday, January 29, 2012 6:21:28 AM
IP Address: 128.178.195.215

© Woodhead Publishing Limited, 2011

(Weitzenböck, 1998) Weitzenböck, J.R., R.A. Shenoi, and P.A. Wilson, Measurement of three-dimensional permeability. *Composites Part A* 29(1–2): 159–169.

(Weitzenböck, 1999a) Weitzenböck, J.R., R.A. Shenoi, and P.A. Wilson, Radial flow permeability measurement. Part A: Theory. *Composites Part A* 30: 781–796.

(Weitzenböck, 1999b) Weitzenböck, J.R., R.A. Shenoi, and P.A. Wilson, Radial flow permeability measurement. Part B: Application. *Composites Part A* 30: 797–813.

(Wietgrefe, 2010) Wietgrefe, M., V. Michaud, M. Sinapius, J. Pariona Lartiga, and K. Schubert, Comparison and evaluation of two different permeability measurement methods for fiber reinforced materials. Submission no. 38, *10th Int Conf on Flow Processes in Composite Materials (FPCM10)*, Ascona, Switzerland, 11–15 July 2010.

(Wolfrath, 2006) Wolfrath, J., V. Michaud, A. Modaressi, and J.-A.E. Månson, Unsaturated flow in compressible fibre preforms. *Composites Part A* 37: 881.

(Wu, 1994) Wu, C.-H., T.J. Wang, and L.J. Lee, Trans-plane fluid permeability measurement and its application in liquid composite molding. *Polym Comp* 15(4): 289–298.

(Wu, 1998) Wu, Y.S., K. Pruess, and P. Persoff, Gas flow in porous media with Klinkenberg effects. *Transport in Porous Media* 32(1): 117–137.

(Yu, 2000) Yu, B.M., and L.J. Lee, A simplified in-plane permeability model for textile fabrics. *Polym Comp* 21, 660–685.

(Zhou, 2006) Zhou, F., N. Kuentzer, P. Simacek, S.G. Advani, and S. Walsh, Analytic characterization of the permeability of dual-scale fibrous porous media. *Comp Sci Technol* 66: 2795–2803.

Copyrighted Material downloaded from Woodhead Publishing Online
Delivered by http://www.woodheadpublishingonline.com
EPFL Lausanne (569-11-299)
Sunday, January 29, 2012 6:21:28 AM
IP Address: 128.178.195.215

© Woodhead Publishing Limited, 2011

Copyrighted Material downloaded from Woodhead Publishing Online
Delivered by http://www.woodheadpublishingonline.com
EPFL Lausanne (569-11-299)
Sunday, January 29, 2012 6:21:28 AM
IP Address: 128.178.195.215